REVIEW

Critical Assessment of Works on Improving Joint Strength of Brazed Cemented Carbides and Steels

Nitin Kumar Sharma[a], Rangasayee Kannan[a], James Hogan[b], Gary Fisher[c], and Leijun Li[a]

[a]Department of Chemical and Materials Engineering, University of Alberta, Edmonton, AB, Canada, T6G 1H9; [b]Department of Mechanical Engineering, University of Alberta, Edmonton, AB, Canada, T6G 1H9; [c]InnoTech Alberta, Edmonton, Alberta Canada T6N 1E4

ARTICLE HISTORY
Compiled April 20, 2021

ABSTRACT
Surface mining causes significant wear damage that affects equipment performance, reliability, and lead to associated downtime costs. To improve the wear resistance of components used in natural resources industries, cemented carbide tiles are joined to engaging surfaces of the components to take advantage of their high hardness, wear resistance, and relatively better strength. Joining of cemented carbide to structural steel can be achieved by various processes, among which brazing is commonly used owing to its relatively simple processing and low cost. A significant challenge in brazing cemented carbide tiles to steels is the poor joint strength. This article aims to review the recent progress in improving joint strength of cemented carbide/steel brazing. **Recent progress on the key factors, including type of filler metals, evolution of joint microstructure, generation of residual stresses, and process parameters have been closely examined and critically analyzed**. The effects of filler metal and joint microstructure on the joint strength and residual stresses are critically reviewed. Future directions of research on brazing cemented carbide tiles to steel in order to improve joint strength have been proposed.

KEYWORDS
Brazing; WC-Co; Steel; Spallation; Shear strength; Interface

1. Introduction

Equipment used in resource-based industries such as natural gas/oil sands extraction and mining undergo severe wear, that affects equipment longevity and reliability. Apart from the equipment loss, there are indirect costs associated with downtime of wear related failures. For applications that are subject to extreme wear conditions as in oil sands and natural gas extraction, companies tend to protect equipment using sintered tiles, owing to their high hardness [1], wear resistance [2–5], and relatively better strength [6]. Carbide, such as WC, particles, typically between 1 to 5 μm in size, held together by a cobalt (Co) or nickel (Ni) matrix alloy, form such sintered tiles. The carbide particles provide the necessary strength and wear resistance, whereas the binding matrix provides the required toughness and ductility [7–10].

Corresponding author: Dr. Leijun Li. Email: leijun@ualberta.ca

Under vibration and impact, cemented carbide composites have low toughness due to the inherent brittle nature of carbides [11–13]. Joining of WC-Co to structural steel is a dissimilar material joining problem [14], involving various joining techniques, including brazing [15–17], diffusion bonding [18–20], fusion welding [21–24], and partial transient liquid-phase bonding [25]. Among the joining techniques, brazing is a commonly used technique for joining cemented carbides to steels, because of its simple processing and relatively low cost. While the relatively low cost of the brazing process is favorable for its use, there are several challenges associated with the brazing of cemented carbides to steel [14]. The greatest challenge is the low strength of the joints, which depends on a multitude of factors, including the choice of filler metal, brazing process parameters, and the magnitude of residual stresses developed [26,27].

Openly published literature on brazing of cemented carbide to steel is limited, or is not disclosing proprietary information. The main objective of this review is to develop a scientific understanding of the metallurgy and process for brazing of cemented carbide with steel for an enhanced joint strength. Both the process parameters for brazing and associated metallurgical changes (microstructural evolution) have been closely examined. Since WC-Co composite is most widely used, the majority of the review will focus on understanding the process/metallurgy of brazing WC-Co/steel, although brazing of other cemented carbides, such as TiC, is also reviewed.

2. Effect of brazing process parameters on joint strength

Table 1 summarises research work conducted on brazing of WC-Co/steel. This table gives the details on composition of alloys (cemented carbide, steel, and filler alloy) used, type of brazing process used, and parameters used for process control. It can be seen that Ag and Cu-based filler alloys with different compositions have been used in most studies. Different types of brazing techniques such as induction, furnace, flame/torch, arc are used to obtain the brazed joints. Depending on the type of brazing process used, important process parameters, which have been studied are temperature, time, voltage and current. Joint strength of WC and steels depends on brazing process parameters (i.e., brazing temperature, brazing time, current, and voltage in case of induction brazing). A summary of selected studies which reported the shear strength values as a function of process parameters for WC-Co/steel brazed joints is given in Table 2. This table details the type of parameter and range in which it was varied during a particular study. In addition, process parameters corresponding to the maximum shear strength are also tabulated.

To visualize the effect of these process parameters, joint strength values from these works are plotted together (Figure 1). All the reports showed an increase in the joint strength with the initial increase in brazing temperature. However, some of these works also showed a decrease in the strength at higher temperatures while the data for even higher temperatures were not available. This shows that there may be an optimum brazing temperature for the highest joint strength. Similarly, with the increase in the brazing time, the joint strength was found to decrease for all the works. These results show that the highest joint strength for brazing at a fixed temperature is generally obtained for relatively shorter brazing time. It should be noted that the absolute value of the highest joint strength for any brazing time - temperature combination is dependent on the composition of cemented carbide, steel and braze filler metal used, as

Table 1. Composition of cemented carbide, steel, and filler alloy, brazing process, and process parameters used in different studies focused on brazing of WC-Co and Steel

cemented carbide	Steel	Filler alloy	Brazing process	Process control	Reference
WC- 10Co	Fe- 0.91C- 1.98Mn- 0.17Si- 0.43Cr- 0.08V	Ag- 20.1Cu- 28.5Zn- 2.0Ni	Induction (Vacuum)	Temperature and time	[26]
WC- 10Co	Fe- 0.21C- 0.4Mn- 0.19Si	Ag- 15.84Cu- 21.52Zn- 8.02Mn- 6.11Ni- 4.12C	TIG	Current, voltage and temperature	[28]
WC- 8Co	SAE1045	Cu– 19.5Ni– 2.5Al	Vacuum furnace	Temperature and time	[29]
WC- xCo-yCr3C2 (x = 4, 8, 13; y = 0.5, 1)	Tool steel (0.45C)	Cu and Ni alloys	Induction	Temperature and time	[30]
WC- 8Co	Fe- 0.325C- 13.43Cr- 0.025Mn- 0.390Si- 0.020S- 0.080Ni	Cu- 38Zn	Vacuum furnace	Temperature and time	[31]
WC- 9Co	Fe- 0.4C- 0.35Si- 0.65Mn- 0.035P- 0.030S	Cu- 41.7Zn- 10Ni- 0.3Si	Oxyacetylene torch	Temperature	[32]
WC- 20Co	Fe- 0.35C- 1Cr- 0.2Mo- 0.2Si- 0.5Mn	Ag- 16Cu- 23Zn- 7.5Mn- 4.5Ni	Induction	Temperature and time	[33,34]
WC- TiC- Co series	Tool steel (0.45C)	Cu-Zn-Ni alloy	Furnace (Ar atmosphere)	Temperature and time	[35,36]
WC- Co	-	Ag- 16Cu- 23Zn- 4.5Ni- 7.5Mn	Furnace (Ar atmosphere)	Temperature and time	[37]
WC- 9.2Co	-	Ag- 20Cu- 29Zn- 0.5Co- 2.0Ni	Induction	Temperature and time	[38–40]
WC- xCo (x = 4, 8, 14)	Tool steel (0.45C)	Cu and Ni alloys	Induction	Temperature and time	[41]
WC- 20Co	16Mn steel	Cu- 4Mn- 38Zn	Vacuum furnace	Temperature and time	[42]
WC- 8Co	SAE1045 steel	Cu and AG- 28Cu	Vacuum furnace	Temperature and time	[43]
WC-Co (B30 grade)	40HM steel	Cu- 10Mn- 3Co	Induction	Temperature	[44]
GE 15	-	W- 26Re	GTA braze	-	[45]
WC-TiC	AISI 4145	AgCuZnCdNi	Oxyacetylene torch	Temperature	[46]
WC- 6Co	4340 Steel	AgCu alloy, Ag, Cu, AuNi alloy	Vacuum furnace	Temperature	[47]
WC	Carbon Steel	Ag- 15Cu- P6	Oxyacetylene and Induction	Voltage, current and temperature	[48]
WC- Co/Ni	410 Stainless steel	CuZn alloy	Vacuum furnace	Temperature and time	[49]
WC- Co	SAE 1045	Cu and C52100 alloy	Vacuum furnace	Temperature and time	[50]
WC- Co	CK 35 Steel	L-AG34Cd and L-AG40Cd	Vacuum furnace	Temperature	[51]

well as type of brazing process. In the absence of joint strength data at higher brazing temperatures and lower brazing times for some of these papers the joint strength reported in them cannot be determined as peak values. The main reasons responsible for these observed variation of joint strength are brazing defects.

Table 2. Range of variations in different process parameters and the maximum joint strength for different studies on brazing of WC-Co and Steel

Process parameter	Braze alloy	Liquidus temperature	Variation	Maximum shear strength (brazing condition)	Reference
Current / Temperature	Ag- 15.84Cu- 21.52Zn- 8.02Mn- 6.11Ni- 4.12C	699 °C	40-100 Amp / 900-1200 °C	289.2 MPa (80 Amp / 1060 °C)	[28]
Time	Cu- 1Zn- 0.7Si and Amorphous Ni- 3.7B- 15.5Cr	1020 °C	600-3600 sec (at 1050 °C)	370 MPa (600 sec)	[30]
Temperature	Ag- 16Cu- 23Zn- 7.5Mn- 4.5Ni	705 °C	710-770 °C (for 30 sec)	366 MPa (770 °C)	[33]
Time	Ag- 16Cu- 23Zn- 7.5Mn- 4.5Ni	705 °C	1-120 sec (at 770 °C)	366 MPa (30 sec)	[33]
Temperature and time	C52100 bronze	882 °C	1080-1120 °C (5-15 min)	358 MPa (1080 °C - 10 min)	[50]
Temperature and time	Cu (99.9 %)	1083 °C	1100-1140 °C (5-15 min)	320 MPa (1140 °C - 15 min)	[50]
Temperature	L-AG40Cd	680 °C	680-730 °C(for 20 min)	91 MPa (730 °C)	[51]
Temperature	L-AG34Cd	680 °C	750-800 °C(for 20 min)	108 MPa (800 °C)	[51]

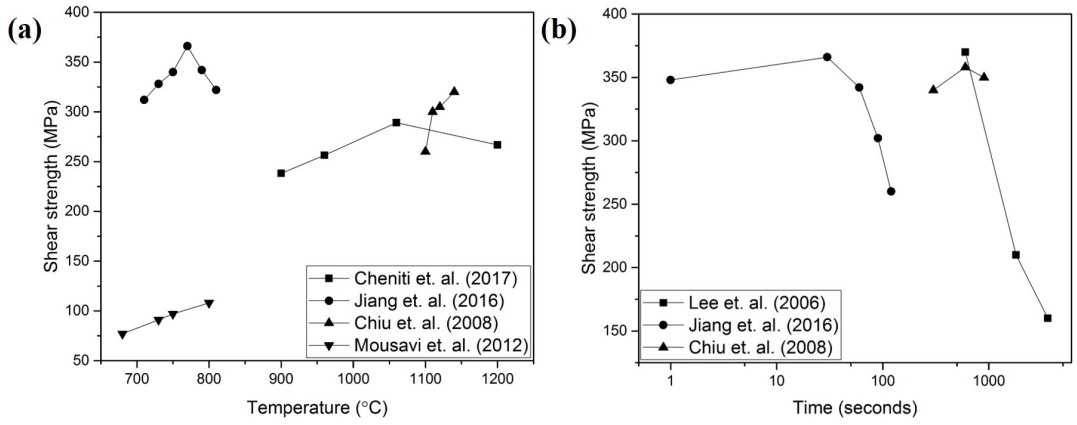

Figure 1. Variation in shear strength of brazed joints as a function of different process parameters; Data from [28,30,33,50,51]

Porosity and cracks at the brazed joints were found to cause a lower joint strength [28]. Figure 2 shows the variation in joint strength and corresponding brazed joint macrographs for different values of current used in a TIG (tungsten inert gas) brazing. A variation of brazing current from 40 A to 100 A resulted in a peak temperature change from 900 °C to 1200 °C. **Joint brazed at the lowest temperature of 900 °C exhibited porosity**. With the increase in peak temperature, **cracks** in the WC-Co/Ag alloy/Steel brazed joint increased. Since **these defects were** only observed

for lower and higher current samples, **we suggest that porosity and cracks were** responsible for the lower joint strength. **While the cracks usually form due to the larger difference in the coefficient of thermal expansion at higher temperatures, the formation of porosity is most likely caused by a lack of wetting at the braze interfaces, resulted from inadequate cleaning, gas entrapment and improper joint clearance**. Although defects can act as one explanation for the observed general trend (an initial increase, followed by a decrease) for the joint strength as a function of process parameters, other microstructural factors may also influence the joint strength. Namely, these factors can include type, fraction and distribution of microstructural constituents [52,53] at the two interfaces (steel/braze and WC-Co/braze), and diffusion of different elements across the interfaces [54,55].

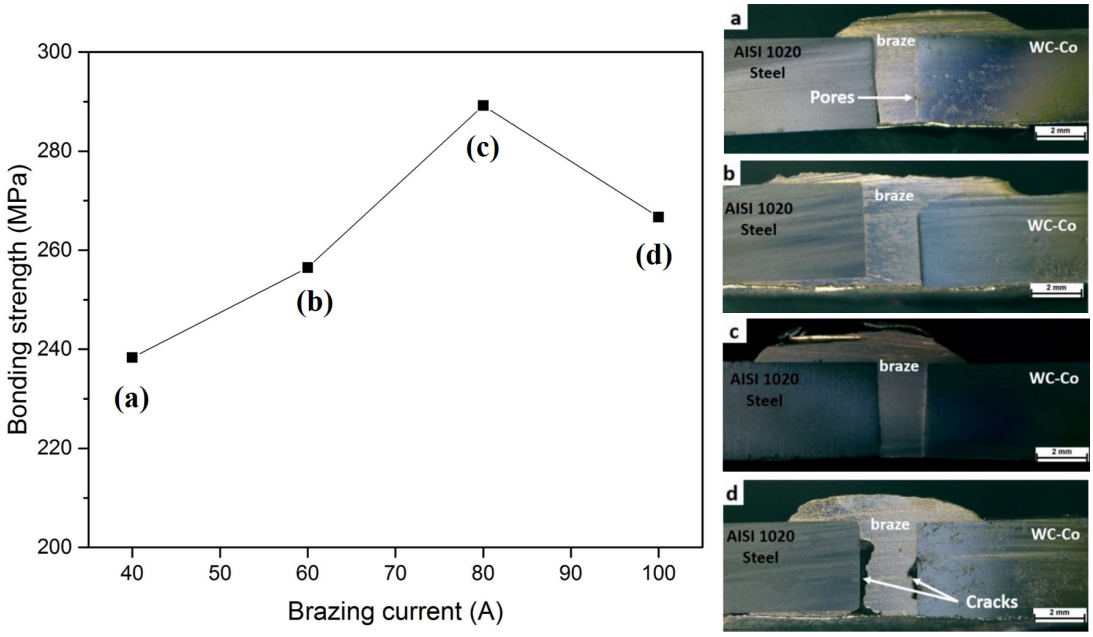

Figure 2. Bonding strength vs brazing current and corresponding transversal sections of WC-Co/AISI 1020 steel brazed joints for different brazing currents: (a) 40A, (b) 60A, (c) 80A, (d) 100A [28]

Formation of brittle intermediate phases and coarsening of WC grains were found to be responsible for lower joint strength at longer brazing times [30]. This is because brazing for longer times at significantly higher temperatures promote grain growth in the braze and diffusion of elements across the interfaces to provide favorable kinetics for the formation of precipitates [56,57]. Brazing of WC-Co and steel using Cu and Ni alloys as filler resulted in the formation of Co_3W_3C precipitate phase [30]. On the other hand, use of Cu and Bronze filler alloys led to the precipitation of Fe-Co-Cu towards the WC-Co/braze interface for both the fillers [50]. This precipitation layer was found to grow in thickness as a function of temperature as well as time before finally connecting both the base materials to result in enhanced bonding. Based on the brazing experiment with Ag-Cd alloy, a higher fraction of Cu-rich solid solution resulted in a higher shear strength [51]. Use of BAg22 alloy as filler was found to result in a reduction in joint strength due to evaporation of Zn from the filler metal, diffusion of Ti from WC/TiC-Co side and the formation of intermetallic compounds, such as Mn_3W_3C, at longer brazing times (as shown in Figure 3) [37]. Diffusion of

Ti towards the braze metal also allowed the formation of stable compounds such as CuTi, $CuTi_2$, $CuTi_3$, Cu_7Ti_2, Cu_3Ti, and Cu_2Ti. Figure 3 shows that 30 minutes of brazing resulted in a thicker diffusion layer depleted in Ti. XRD scan shows the presence of intermetallic compound Mn_3W_3C resulted from 20 minutes of brazing.

All these observations for different system of cemented carbide and braze filler alloys point towards significant microstructural changes in the vicinity of the braze joint responsible for resulting joint strength.

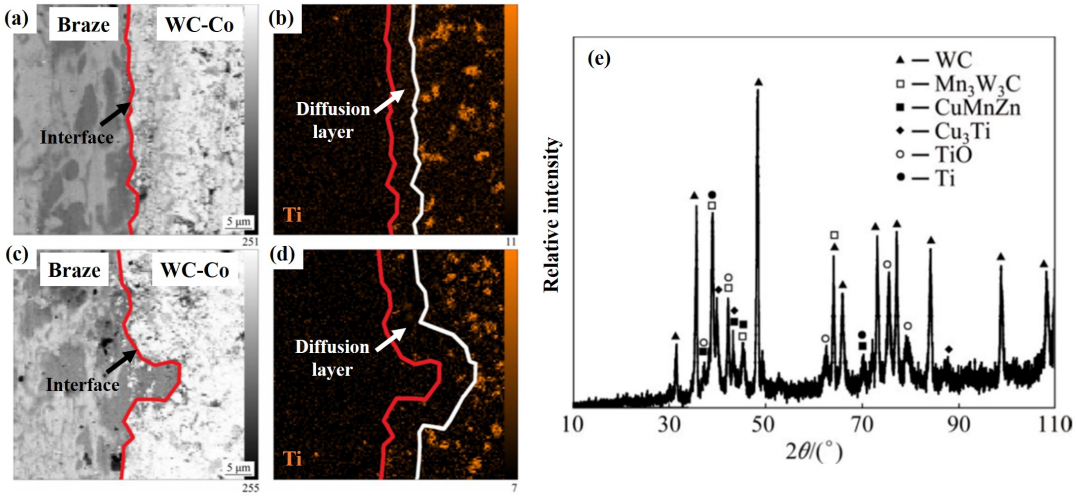

Figure 3. SEM images (a, c) and EDS elemental maps (b, d) of joints brazed at 730 °C holding for 15 min (a, b) and 30 min (c, d); (e) XRD pattern of joint brazed at 730 °C for 20 min with filler alloy of 250 μm in thickness [37]

Figure 4 shows the microstructure obtained near the braze of a WC-20Co/Ag-Cu alloy/35CrMo steel brazed material as a function of brazing temperature [33]. In the case of Ag-Cu filler alloy, there is a dark etched Cu-rich solid solution present at the reaction layer on either side of the braze (i.e. braze/WC-Co and braze/steel interface, labeled as A and E arrows respectively) in all the braze conditions. The braze consists of a uniform distribution of three different phases, viz., dispersion of Ag-rich solid solution (white color, arrow B), Cu-rich solid solution (black color, arrow C), and eutectic between Cu and Ag (arrow D). It can be seen that with the increase in peak temperature, the fraction of Cu-rich solid solution dispersed in the matrix of the braze decreases. In addition, with the increase in brazing temperature, a reaction layer is developed as a result of Co migration from the WC-Co towards the braze resulting in enrichment of Co closer to the braze/WC-Co side as shown in Figure 5. Thus, it is clear that with the increase in brazing peak temperature, the amount of Cu-rich solid solution in the braze decreases, and there is an enrichment of Co/migration of Co from the WC-Co side towards the braze. This reaction sequence resulted in an initial increase in joint strength, followed by a drastic reduction in joint strength as shown earlier in Figure 1 and Table 2. Similar changes in microstructure near the braze interface were observed while varying the brazing time at a particular temperature [33,50]. Again, the reduction in Cu solid solution and Co migration into the reaction layer at WC-Co/braze interface was attributed to the observed trend in joint strength.

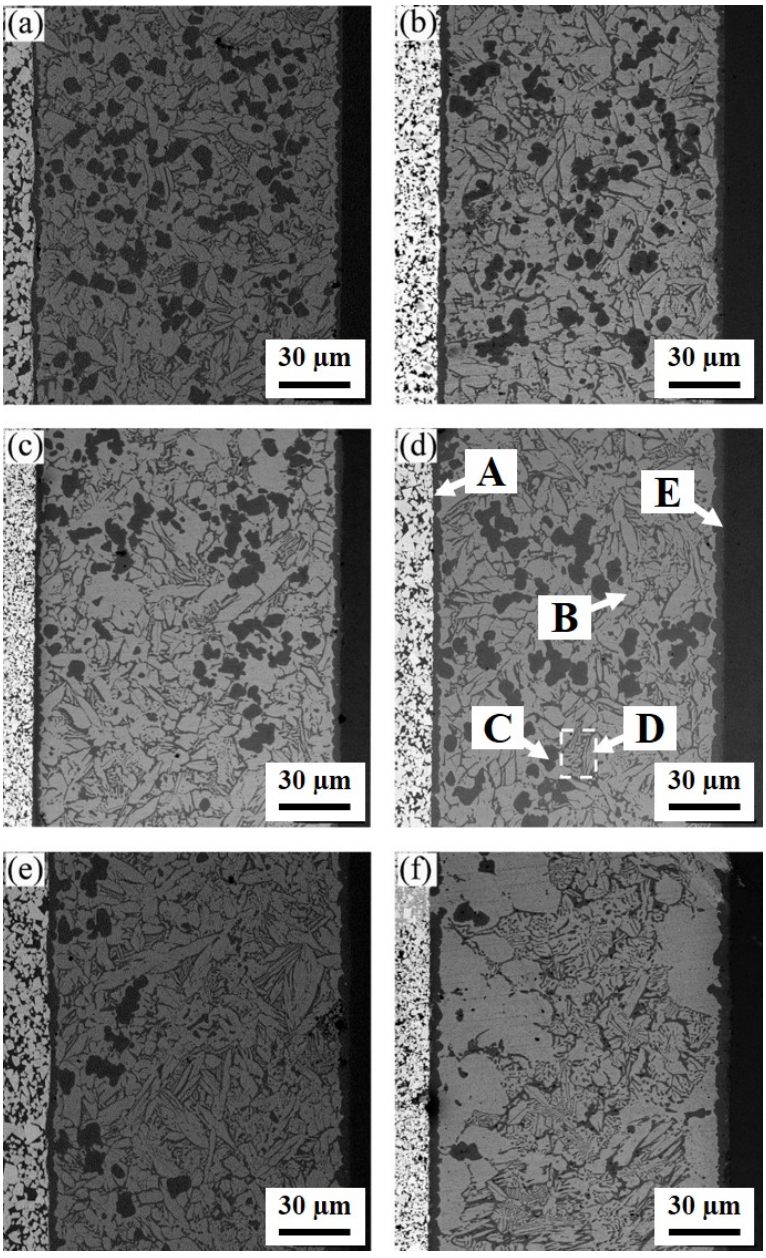

Figure 4. Backscattered electron images of the weld bead brazing for 30 s at: (a) 710 °C, (b) 730 °C, (c) 750 °C, (d) 770 °C, (e) 790 °C, and (f) 810 °C [33]

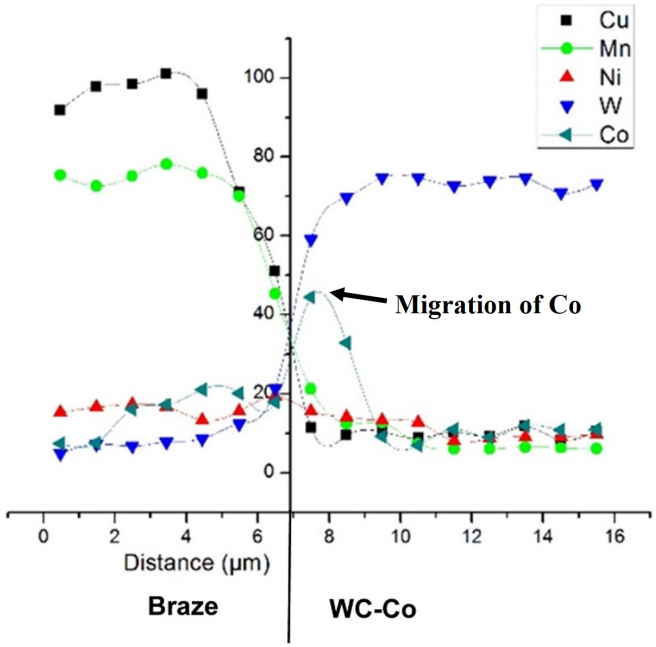

Figure 5. Distribution of major elements across the brazed joint measured using EDS [33]

Since gap between the faying surfaces to be joined, also known as joint clearance, affects the joint strength, filler alloy thickness is also expected to have a role in determining the quality of the brazed joint. In the case of thinner filler alloy or indirectly the lower values of joint clearance (typically lower than 0.006 in or 150 μm), there is an increased possibility of suppressed capillary action and hence a possibility for a non-uniform flow of filler metal through the joint. **In case of very thin filler alloy, the volume of molten filler is also very small, which may lead to an inadequate flowability. Smaller gap between the base materials only allows a stagnant flow of molten filler throughout the brazed joint, resulting in the under-filling of the joint and the formation of joint defects [37,58,59]**. Thinner filler alloy or lower volume of molten filler also means lower brazed joint thickness. Joint strength corresponding to a low braze thickness is generally higher, and sometimes reaches the strength of base metal. **We believe this is because of the suppressed necking due to a very thin layer of filler metal. Braze joint, in this case, experiences a triaxial state of stress. High values of triaxial tensile stresses were proved to have increased the joint tensile strength [60–62]. In contrast, joint strength for thicker brazed joints would be lower due to a reduction of constraints from the base metal**. Joint strength, in this case, drops significantly and eventually reaches the lower strength values of the filler metal. Hence, in order to obtain a stronger brazed joint, the filler metal thickness should be optimized to provide the balance between the uniform flow of filler metal and joint strength.

The effect of filler metal thickness of BAg22 filler alloy on the joint strength of WC-Co/Steel joints is shown in Figure 6 [37]. Brazing temperature and time were kept fixed to evaluate the standalone effect of filler thickness on the joint strength. Brazing temperature was fixed at the recommended brazing temperature for BAg22

(730 °C). **The resulting strength of the brazed joint was found to increase with a filler thickness between 50 and 250 μm. We believe with a relatively thicker filler alloy (average 150 μm) there was a better capillarity action and hence better flow of filler metal during brazing. This thickness of brazing might also have generated beneficial reactive wetting [63–65] and migration of elements enhanced wetting [66,67]. We believe the lower shear strength of the thicker filler metal (400 μm) must be due to the reduced base metal constraints or loss of triaxial stress state during the testing**.

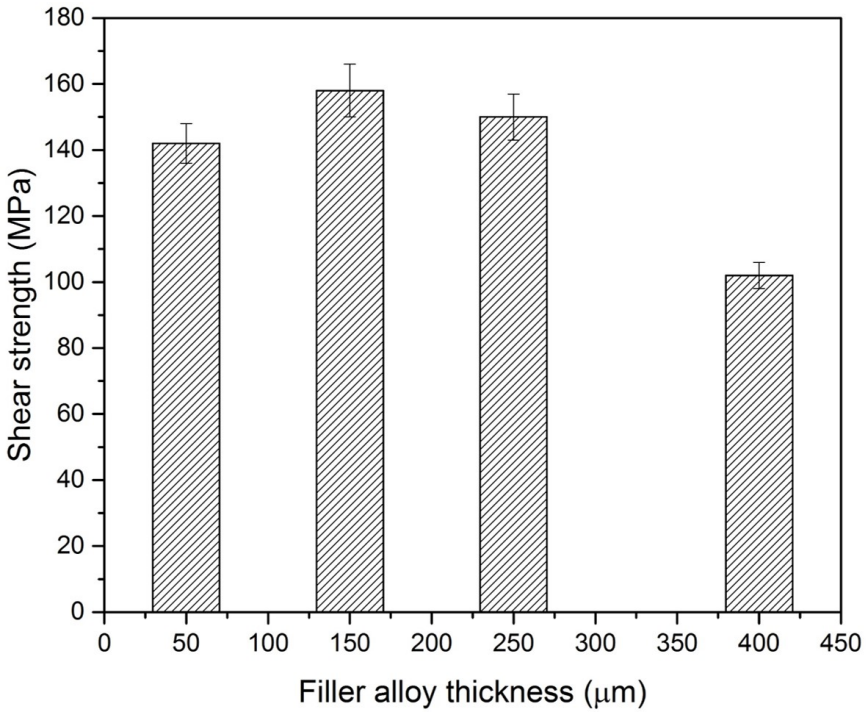

Figure 6. Effect of filler alloy thickness on shear strength of joints brazed at 730 °C for 15 min. Data from [37].

Before brazing, there is a difference in the concentration of elements such as W, C, Co, Cu, Zn etc. across the WC-Co, braze and steel regions. Owing to the high concentration gradients and enough thermal activation at the brazing temperatures, diffusion of these elements would occur very easily across the two interfaces. Although the migration of these elements helps in wetting the base materials, local segregation of these elements could also lead to the formation of brittle intermetallic phases. While the insufficient migration of elements would lead to inadequate wetting, excessive migration also leads to preferential movement of elements to form intermetallic compounds and result in poor wetting [68–70]. Hence formation of intermetallic compounds should be avoided in order to improve the wetting properties.

The selection of suitable flux is an important factor to overcome the problems associated with the insufficient migration of elements. Use of flux helps to achieve good wetting characteristics. Flux is generally a mixture of complex compounds that melts before brazing filler to form a protective layer for the molten braze and helps in removing the oxides from the substrate, and thus

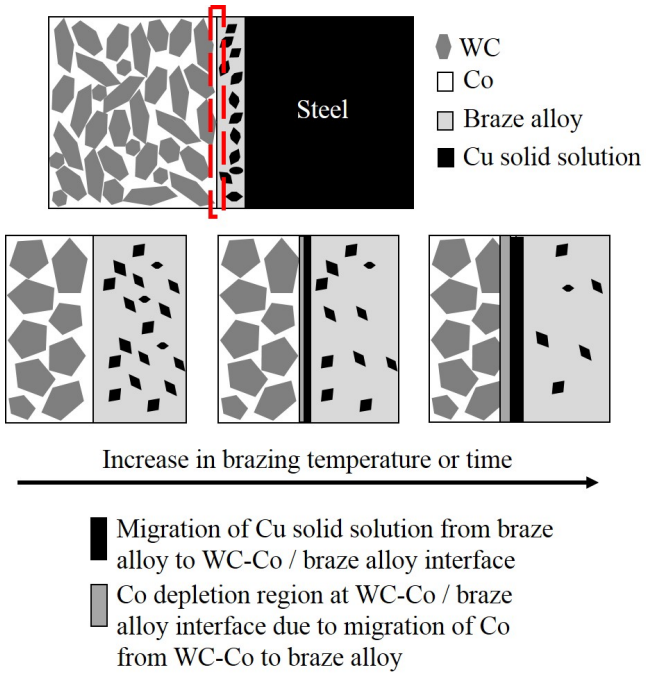

Figure 7. Schematic showing the effect of brazing temperature or time on the microstructure of brazed WC-Co/Steel joint.

improving the wetting [71]. **Selection of flux depends on the composition of base materials and filler metals, as well as the brazing temperature. For example, aluminum and magnesium alloys utilize aluminum or magnesium-based fluxes containing fluorides, whereas silver-based fluxes containing compounds of boric acid and potassium borates are used for materials prone to oxidation at brazing temperatures such as ferrous, nickel and cobalt-based alloys**. Intermetallic phases could become the preferential sites for crack nucleation during loading and hence have a deleterious effect on the joint strength [30]. As discussed earlier, some of these intermetallic phases for different filler systems include Co_3W_3C, Mn_3W_3C, CuTi, $CuTi_2$, $CuTi_3$, Cu_7Ti_2, Cu_3Ti, and Cu_2Ti. Since longer times at suitably high temperatures would result in thermodynamic stabilization of these phases, higher brazing times should be avoided. On the other hand, lower temperatures and/or lower brazing times may not allow enough migration of elements for effective wetting.

The general effect of brazing temperature/time on the joint properties for Ag-Cu based fillers can be summarized by the schematic shown in Figure 7. Diffusional migration of elements such as Cu and Co near the cemented carbide-braze interface can be clearly visualized from this figure. It is suggested that a too low brazing temperature/time will result in a lower joint strength between the braze and WC-Co/Steel, whereas a too high brazing temperature/time will result in the reduction of solid solution in the braze and migration of Co from WC-Co towards the braze, also leading to a poorer joint strength. It is, hence, clear that the brazing temperature and time have to be optimized in a way to obtain high Cu solid solution and avoiding the migration of Co. This optimization should be done for a given brazing process to achieve superior joint strength.

3. Effect of braze filler metals on joint strength

Filler metals play an important role in brazing cemented carbides to steel. The thermal expansion coefficient of cemented carbide (typically of the order of 5.5×10^{-6} K^{-1} to 9×10^{-6} K^{-1}) is half that of steel (typically of the order of 10×10^{-6} K^{-1} to 20×10^{-6} K^{-1}). The filler metal for the brazing process must be chosen in such a way that the coefficient of thermal expansion of the braze filler metal has to be at an intermediate value in comparison to the cemented carbide and steel to minimize the internal thermal stresses [26,27].

Besides the thermal expansion coefficient, the filler metal must have a superior wettability at the brazing temperature [62]. Wettability of filler metals is generally characterized by the wetting angle, which is strongly dependent on the interfacial energies between the base material-molten filler metal, base material-brazing atmosphere, and the molten filler metal-brazing atmosphere. A wetting angle lower than 90° implies proper wetting of base materials by the filler metal. Because the surface tension is affected by the temperature, selection of suitable brazing temperature is important for a given filler metal. The addition of alloying elements to the filler metal would influence the wetting behavior. Proper flow and wetting ensures the joint is defect-free, which also improves the joint strength [62]. Composition of the filler metal also influences the diffusion behavior of different alloying elements across the base materials and braze. Since the interdiffusion behavior determines the evolution of microstructure, especially the formation of brittle intermetallic phases at the braze interface, composition of the filler metal has an important role on the microstructure and strength of the joint.

Typically used filler metals for brazing cemented carbides to steels include a combination of Ag, Cu, Zn, Mn, Ni, and Al, with Cu and Ag being the matrices of the braze. Cu-based filler metals include Cu-Zn, Cu-Zn-Ni, and Cu-Sn-Ni systems [30,35,36,50,72,73], whereas Ag-based filler metals include Ag-Cd and Ag-Cu-Zn-Mn-Ni-Co systems [28,33,51,74–77]. Considering the increase in the use of Ag-based commercial filler metals, especially BAg22 and BAg24, in this review, special attention is given to these two filler metals. Figure 8 shows the liquidus surface for the ternary Ag-Cu-Zn system. Compositions of both BAg22 and BAg24 lie close to the 700 °C liquidus section but with BAg22 solidifying in primary Ag solid-solution and BAg24 solidifying in the intermediate β solid-solution. The effect of the filler metal composition on the joint strength of WC-Co/steel joints brazed using BAg22 and BAg24 will be discussed. Nominal chemical compositions and physical properties of BAg22 and BAg24 filler metals are shown in Table 3 and Table 4.

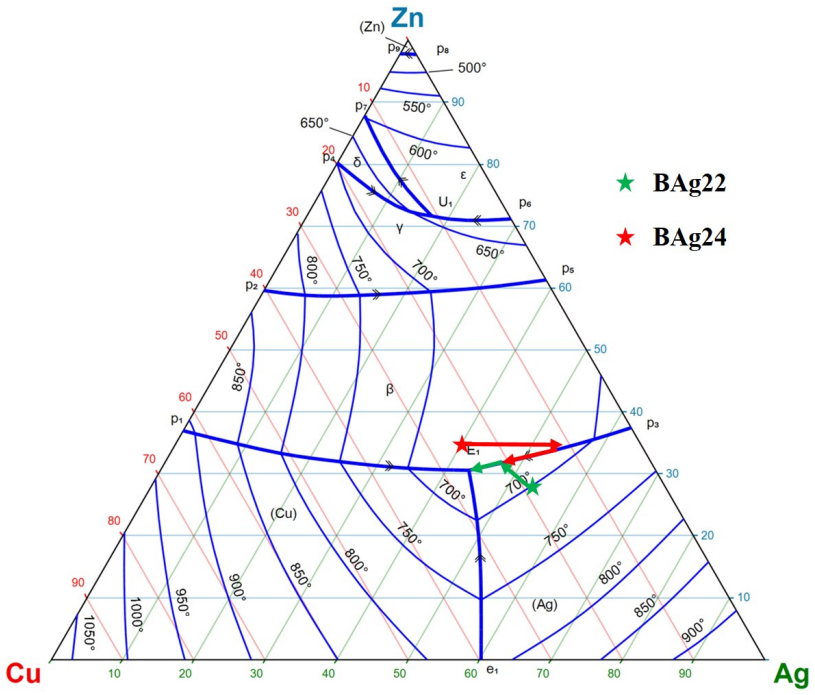

Figure 8. Liquidus surface for ternary Ag-Cu-Zn system along with typical solidification paths for BAg22 and BAg24 alloys [78]

Table 3. Nominal chemical composition (Wt. %) of BAg22 and BAg24 filler metals [79,80]

Filler Alloy	Ag	Cu	Zn	Mn	Ni	Other elements
BAg22	49±1	16±1	23±2	7.5±0.5	4.5±0.5	0.15
BAg24	50±1	20±1	28±2	-	2.0±0.5	0.15

Table 4. Thermophysical properties of BAg22 and BAg24 filler metals [79,80]

Property	BAg22	BAg24
Color	Yellow White	Yellow White
Solidus (°C)	680	660
Liquidus (°C)	699	707
Recommended brazing temperature (°C)	726-754	735-762
Density (Troy Oz./inch^3)	4.68	4.83
Specific gravity	8.88	9.17
Electric conductivity (%IACS)	5.70	15
Electric resistivity ($\mu\Omega$-cm)	30.30	11.90

The major difference between the two filler metals is the amount of Mn and Ni. While BAg22 has significant additions of Mn (7.5 wt. %) and Ni (4.5 wt. %), BAg24 does not have any Mn added and has only half the Ni content as BAg22. In comparison to BAg22, BAg24 has a lower solidus and higher liquidus temperature, and hence has a larger width of mushy zone. In addition to the low amount of Mn and Ni, BAg24 also has higher amount of Ag and Cu (in comparison to BAg22), which increases the ductility of the filler alloy, thereby reducing the internal stresses developed during the brazing process [62].

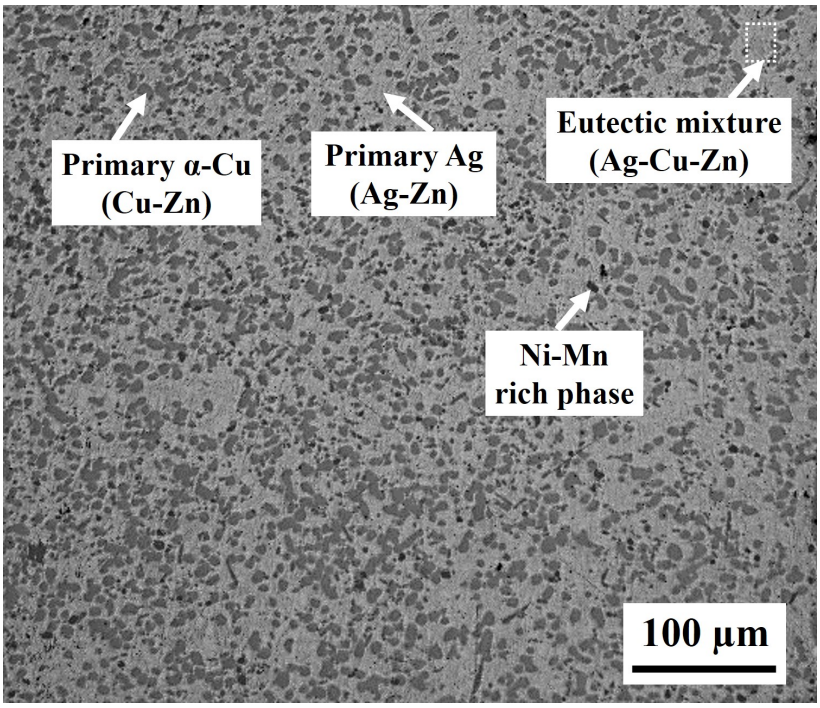

Figure 9. Representative SEM micrograph of BAg22 filler alloy showing three distinct phases, rich in Cu, rich in Ag, and rich in Ni-Mn

The typical microstructure of an Ag based braze, as shown in Figure 9, consists of primary α-Cu solid-solution, primary Ag solid-solution, Ni-Mn rich phase, and eutectic mixture of Ag-Cu-Zn, each exhibiting a different etching response. Difference in composition of BAg22 and BAg24 leads to a difference in the relative fraction of these different phase constituents, thus also affecting the properties of the joint. The addition of Cu to Ag-based filler metal results in the formation of higher fraction of fine Cu-rich phases. These phases improve the joint strength through dispersion strengthening [33].

Addition of each element to the existing filler alloys changes the solidus and liquidus of filler alloys and hence it would also have a unique effect on the brazed characteristics. Table 5 shows the effect of addition of small amounts of Co and Ni to BAg24 filler alloy on the solidus and liquidus temperature ranges. While the addition of Co has a very small effect on solidus and liquidus temperatures, addition of Ni leads to an increase in the liquidus temperature.

Table 5. Chemical composition (Wt. %), solidus, and liquidus temperature of BAg24 filler metal with varying Ni and Co content [40]

Ni-Co	Ag	Cu	Zn	Co	Ni	Solidus (°C)	Liquidus (°C)
0Ni-0Co	50-52	19-21	28-30	-	-	673-678	697-702
2Ni-0Co	49-51	19-21	27-29	-	2.0	671-676	699-704
0Ni-0.5Co	50-52	19-21	27.5-29.5	0.5	-	673-678	698-703
2Ni-0.5Co	49-51	19-21	26.5-28.5	0.5	2.0	672-677	706-709

Microstructures shown in Figure 10 show that adding Ni to BAg24 filler metal resulted in the formation of α-Cu solid solution phases along the interface. The presence of α-Cu solid solution phase was confirmed by the EDS elemental scan from dark col-

ored phases in the microstructures (Table 6). Consequently, the distribution of Ag and Co elements across the interface continuously changed. The continuous distribution of Ag and Co elements across the interface caused the wetting characteristics to improve as shown in the micrographs.

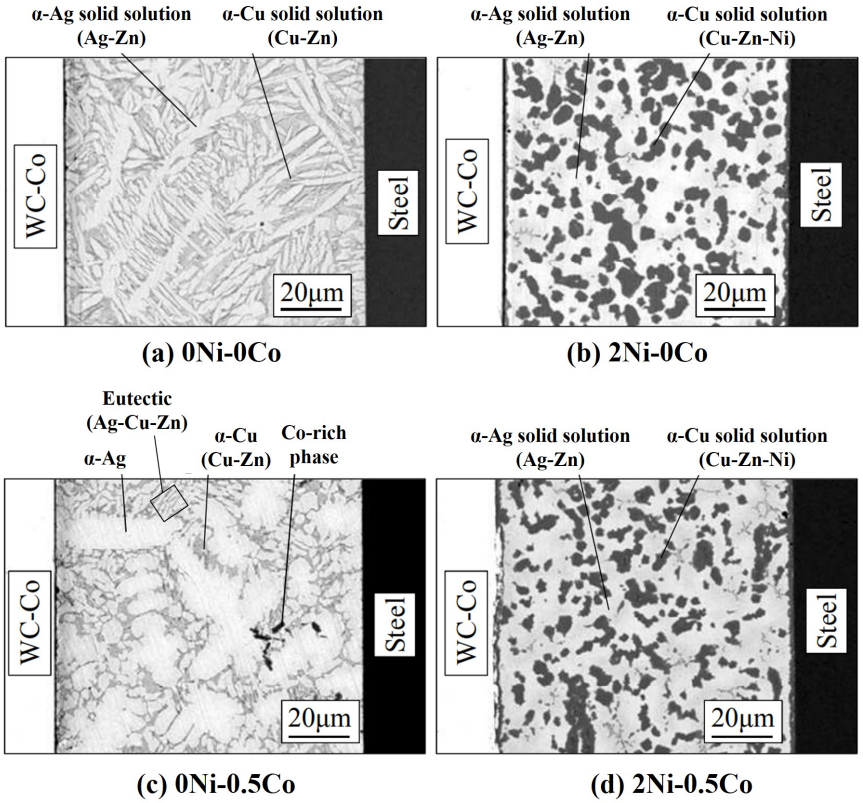

Figure 10. SEM Micrographs of BAg24 filler metal alloyed with various Ni and Co levels [40]

Table 6. EDS results (at.%) from specified position in Figure 10 [40]; W, G, D, and B are white, grey, dark, and black colored phases respectively

region	Ag	Cu	Zn	Ni	Co	W	Fe
0Ni-0Co (W)	56.26	15.73	26.95	-	0.13	0.75	0.13
0Ni-0Co (G)	25.07	41.43	31.09	-	0.05	0.48	0.08
2Ni-0Co (W)	67.88	10.35	17.44	0.64	0.07	1.42	0.18
2Ni-0Co (D)	2.74	41.74	30.61	23.43	0.10	0.86	0.31
0Ni-0.5Co (W)	58.93	15.17	25.06	-	-	0.73	0.08
0Ni-0.5Co (G)	36.48	34.28	27.99	-	0.16	0.95	0.10
0Ni-0.5Co (B)	1.01	2.21	3.36	-	90.93	0.52	1.88
2Ni-0.5Co (W)	72.73	10.68	14.81	0.67	0.15	1.30	-
2Ni-0.5Co (D)	2.65	40.87	29.22	23.04	3.41	0.68	0.09

A schematic representation of the Co concentration distribution across the interface of the WC-Co and brazed layer as determined using EDX elemental scans, along with the variation of Co depletion zone is shown in Figure 11. The addition of Ni is suggested to enhance the inter-diffusivity of Co, resulting in an increase in width of the Co depleted zone. The addition of Ni also results in the formation of coarse Cu-rich solid solution at the WC-Co/braze and braze/Steel interfaces. However, the addition of Co

into the filler metal lowers the concentration gradient of Co across WC-Co and braze. The addition of Co reduces the extent of diffusion from WC-Co to braze and hence also reducing the width of the Co depleted zone. Hence the addition of Co also inhibits the formation of any Co containing intermetallic phases. Figure 12 shows the effect of Ni and Co addition to the filler metal on the joint strength. **Since the addition of Co leads to lower width of the Co depleted zone, it also results in the improvement in the joint strength even though there is a large scatter in data [40]. Although the addition of Co improves the joint strength, the addition of Ni and hence the wider Co depletion zone at the interface of the joint resulted in unchanged joint strength values within the statistical scatter**.

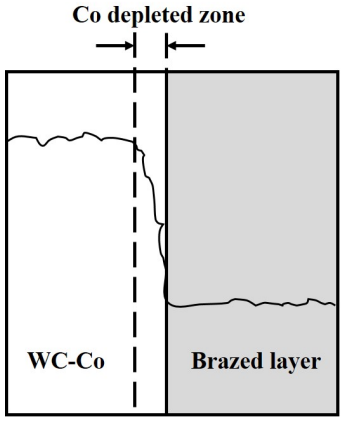

Filler composition	Width of Co depleted zone
0.5 Co – 0 Ni	0.2 µm
0 Ni – 0 Co	0.5 µm
0 Co – 2 Ni	0.9 µm
0.5 Co – 2 Ni	1.4 µm

Figure 11. (left) Schematic of Co concentration across the interface of WC-Co and brazed layer; (right) typical variation in the width of Co depleted zone based on EDS results of Co element around interface of brazed joints using a 0.5Co-0Ni, 0Co–0Ni, 0Co-2Ni and 0.5Co-2Ni. Data from [40]

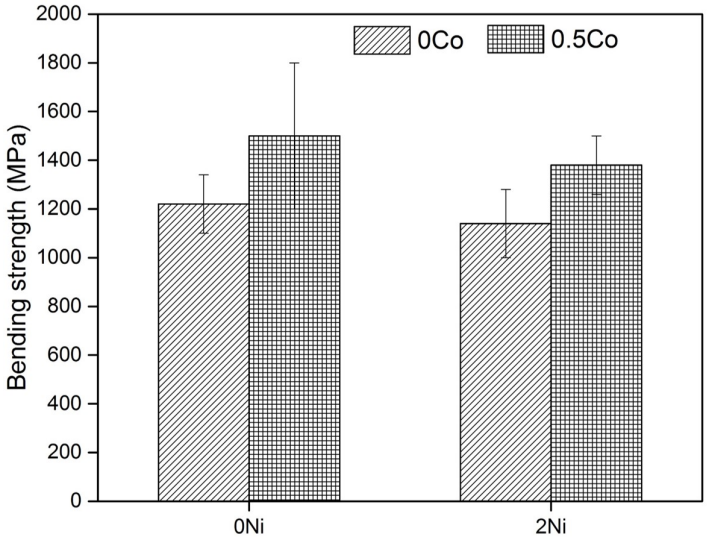

Figure 12. Bending strengths of brazed joints using 0Ni–0Co, 0Ni–0.5Co, 2Ni–0Co and 2Ni–0.5Co. Data from [38]

Although BAg22 and BAg24 are the most popular filler alloys for brazing cemented carbides to steels, alloying addition to these filler alloys presents new opportunities for enhancing the joint strength. Each of the alloying elements in the braze serve a particular function in improving the joint strength:

(1) Cu and Ag serve the purpose of reducing the residual stress levels generated during the brazing process due to their inherently higher ductility [81,82].
(2) Co decreases the concentration gradient across WC-Co and braze. This leads to decrease in the extent of Co diffusion and hence inhibiting the formation of Co containing intermetallic phases [83,84].
(3) Ni serves the purpose of increasing the inter diffusivity with Fe and Co, thereby resulting in a better joint strength [49,85].
(4) Ni, Al, and Zn increase the wettability and lower the liquidus temperature of the braze. However, a high Al content will result in formation of intermetallics, which may lead to a reduction of joint properties [86].

Recent developments: Braze fillers for TiC-Ni based cemented carbides- While WC-Co is the most widely used cemented carbide for wear resistant application owing to their favorable mechanical properties and availability, TiC-Ni based cemented carbides are gaining popularity as a suitable substitute for wear resistant applications. Though there are not much work with regards to filler metals for brazing of TiC to steel, a recent review conducted by Way et al. [62] suggested CuNiMnNb system as a potential candidate for brazing TiC to steel. A brazing temperature of 1170 °C and a brazing time of 15 minutes for brazing TiC to steel using Cu55– Ni32– Mn5– Nb8 (wt. %) filler yielded highest joint strength as shown in Figure 13 [87]. **Highest joint strength for TiC/Steel system in Li's work was around 95 MPa [87], while that for WC-Co/Steel system by Cheniti et. al. was around 290 MPa [28]. This shows that strength of joints brazed with TiC-Ni is far inferior as compared to WC-Co**.

The joint strength for TiC-Ni based cemented carbides also follows the similar trend as discussed earlier for WC-Co based cemented carbides. Strength of the brazed joint increases with an initial increase in the brazing temperature. However, there is a decrease in joint strength upon further increase in brazing temperature due to the formation of intermetallic compounds [87]. Similarly, higher brazing times allowed for the diffusion of elements across the interfaces and resulted in the formation of intermetallic compounds, leading to weaker joints.

Figure 14 shows the microstructural observations for the TiC cemented carbide to steel brazed joint. The concentration of different elements across the brazed joint is shown in Figure 14b. Nb in the filler metal was found to be an active element [87]. The diffusion of Nb from the filler metal and C from the TiC results in the formation of αTi solid solution at the braze TiC interface (transition zone shown in Figure 14c). Similarly, this also resulted in the formation of Nb_2C/Nb_6C_5 (Figure 14d), both of which have a higher thermodynamic tendency to form at the brazing temperature range (Figure 14e).

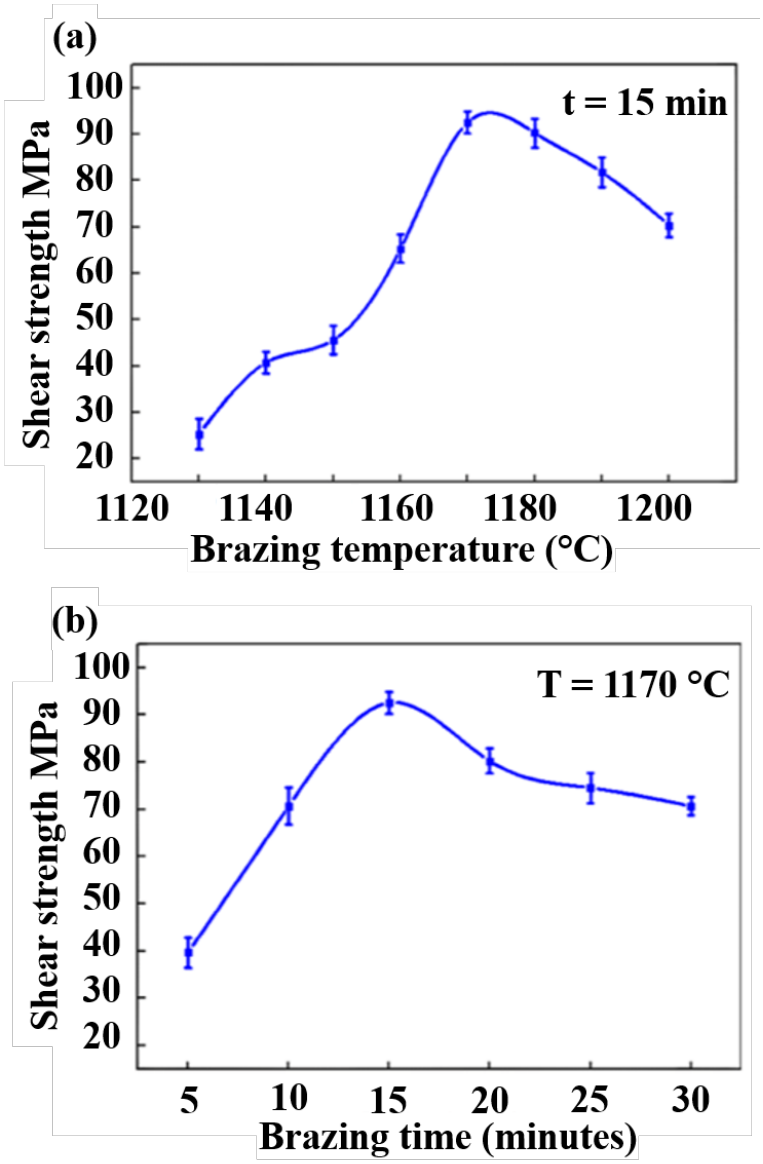

Figure 13. Shear strength of joints brazed (a) at various temperature for 15 min; (b) at 1170 °C for various holding time [87]

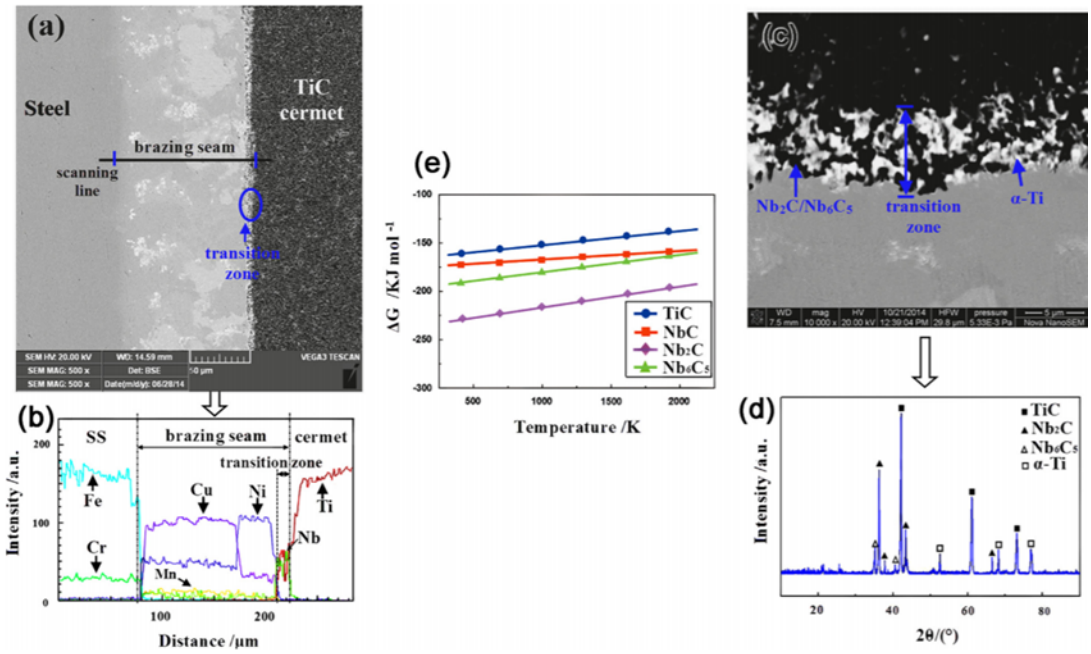

Figure 14. Analysis of brazed joint: (a) SEM morphology; (b) elemental concentration profile corresponding to (a); (c) magnified of blue circle in (a); (d) XRD for transition zone;(e) ΔG for carbides changes with temperature [87]

Other experimental filler metals for brazing TiC to steel include amorphous based filler metals produced by rapid solidification. Laansoo et al. [88,89] developed a series of amorphous filler metals and identified their brazing temperature range and joint strength and compared it with traditional filler metals and found that the amorphous filler metals exhibited a higher joint strength in comparison to the Cu/Ni/Mn based traditional filler metals. The results of their study are shown below in Table 7. It can be seen from Table 7 that amorphous filler metals have shear strength much greater than the traditional filler metals used for brazing TiC-Ni cemented carbides to steels. **Although amorphous filler metals are still in development and are not commercially available, amorphous filler metals have shown some promise in brazing of not only TiC-Ni cemented carbides to steel, but also other alloy systems, including ceramics [90–92]**. It is believed that the higher internal energy of metastable amorphous filler metals contributed to the decrease in brazing temperature and improvement in wettability. The formation of intermetallic compounds was also suppressed in case of amorphous filler metals which led to increase in joint strength [93]. Further investigations into the development of amorphous filler metals and their role in enhanced joint strength as compared to traditional alloys, are required.

Table 7. Chemical composition, brazing temperature, brazing atmosphere, shear strength of amorphous filler metals (AFM) compared with traditional filler metals (TFM) [88,89]

Grade	Type	Composition	Brazing T (°C)	Atmosphere	Shear Strength (MPa)
S1201	AFM	52Ti-24Cu-12Zr-12Ni	920	Vacuum	260
S1204	AFM	72Cu-28Ti	1020	Vacuum	300
S1311	AFM	70Ni-16Co-5Fe-4Si-4B-0.4Cr	1030	Vacuum	200
MBF20	AFM	82Ni-7Cr-4Si-3B-3Fe	1070	air	220
Argo Brass 49H	TFM	40Ag-16Cu-23Zn-7.5Mn-4.5Ni	690	air	190
F-Bronze	TFM	58Cu-38Zn-2Mn-2Co	910	air	200

4. Type of binder in cemented carbides

The amount of binder in the cemented carbides influences the thermophysical properties of the cemented carbides and hence is expected to affect the joint strength. Figure 15 shows the effect of different Co content (binder) on the joint strength [41]. Lower joint strength was found for higher brazing times for all the different Co content systems. Increase in Co content from 4% to 8% was found to result in the increase in joint strength. However for 10% Co content, the joint strength was found to decrease. Lower joint strength at higher brazing times was atrributed to the growth of WC particles, formation of brittle Co_2Cr_3 intermetallic compound, and linear shape of braze/steel interface. Non-linear shape of the interface, observed at lower brazing times as well as 8% Co sample, increased the overall area of the interface which led to increase in joint strength [41].

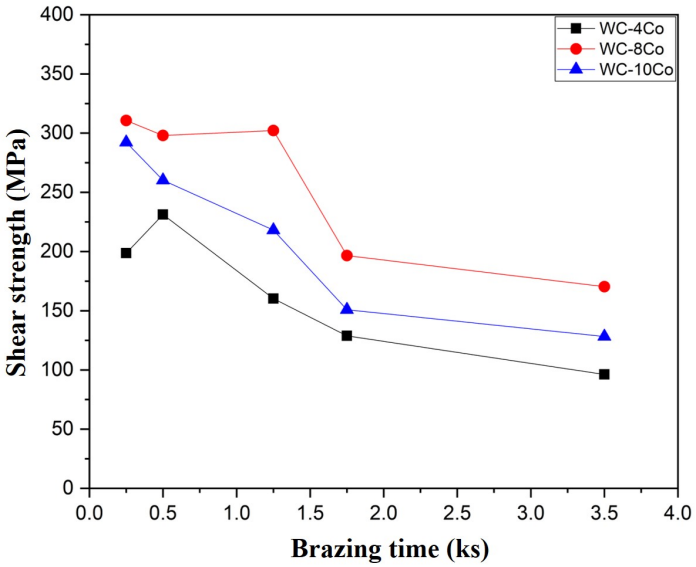

Figure 15. Effect of Co in the binder on the shear strength of brazed joint as a function of brazing time. Data from [41].

Varying Cr_3C_2 and Co addition in the binder to WC-Co was found to result in the formation of η phase at higher brazing times [30]. It was claimed that with the increase in brazing time and decrease in Cr_3C_2 addition, the amount of η phase increases, as shown in Figure 16. This results in an increase in joint strength initially with the increase in Cr_3C_2 content, but a decreased joint strength when Cr_3C_2 is increased to

1%, as shown in Figure 17. Initial increase in the joint strength with the increase in Cr_3C_2 content was attributed to the inhibition of the formation of η phase. However, for even higher Cr_3C_2 content, Cr_7C_3 carbides were formed which led to decrease in the joint strength. The highest joint strength was found in case of 8% Co content in WC. This is due to the observation of linear interface between braze and steel for lower and higher Co contents. As explained before, linear shape of the interface led to lower joint strength due to lower interface area. With the controlled addition of Cr_3C_2 content, an increase of 60 MPa was observed in joint strength as compared to no addition of Cr_3C_2 [30,41].

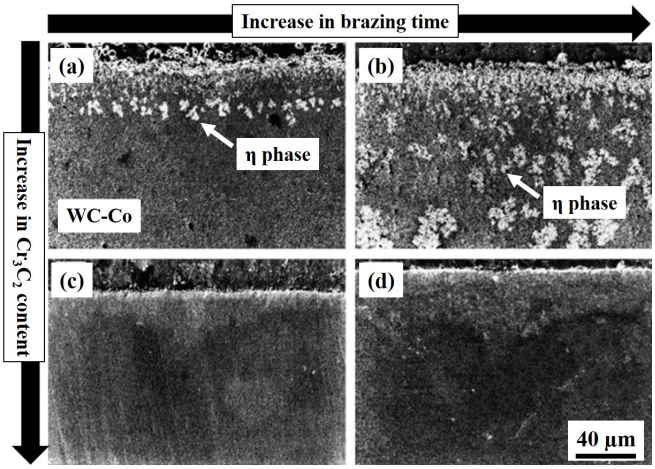

Figure 16. SEM micrographs of WC–Co part near the interfacial layer representing effects of Cr_3C_2 on g phase morphology with brazing time at 1323 K: (a) 0.6 ks and (b) 3.6 ks: WC–8%Co/carbon steel, (c) 0.6 ks and (d) 3.6 ks: WC–8%Co + 0.5%Cr3C2/carbon steel [30]

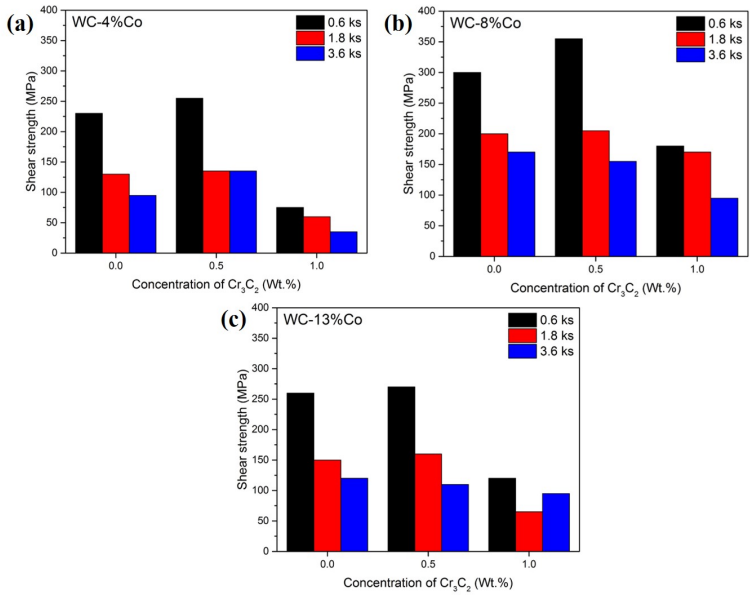

Figure 17. Shear strength with the concentration of Cr_3C_2 and brazing times: (a) WC–4%Co, (b) WC–8%Co and (c) WC–13%Co at 1323 K. Data from [30]

As mentioned earlier, with the increase in Cr_3C_2 content, the formation of Cr-rich Cr_7C_3 carbides in the joint was observed as shown in the XRD patterns in Figure 18, where characteristic Cr_7C_3 peaks are observed at increased brazing time, which results in a reduction in shear strength of the joint. Cr and Co rich M_7C_3-type carbides results in deterioration of mechanical properties. Formation of these carbides is affected not only by the addition of Cr_3C_2, but also Co content in the WC [30]. This is the reason why the Cr_3C_2 content should be added in a controlled manner depending on the Co composition of WC to achieve the optimum mechanical properties of the joint. In summary, it can be said that the addition of different constituents as binder in WC or TiC results in microstructural changes, especially the formation of η phase and Cr-rich Cr_7C_3 carbides. These changes in the microstructure influence the joint strength. This understanding provides an initial point for further investigations into the phase transitions near the brazed joints.

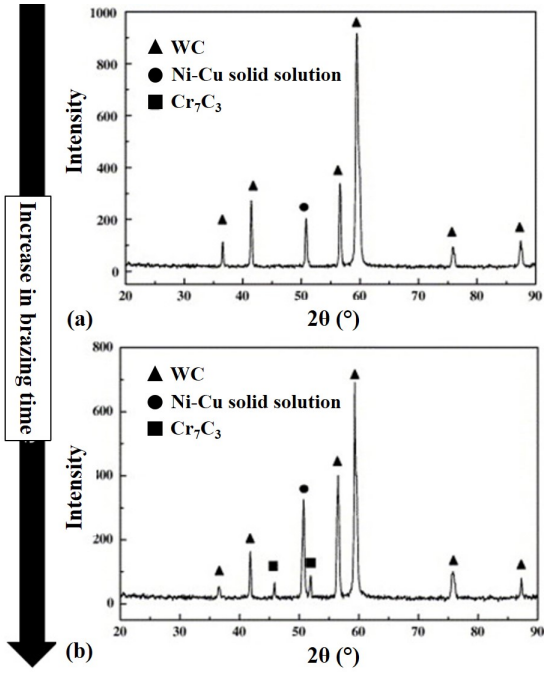

Figure 18. XRD analysis of interfacial layer for WC–8%Co + 0.5% Cr_3C_2/ insert metals/carbon steel joints at 1323 K for (a) 0.6 ks and (b) 3.6 ks [30]

5. Effect of residual stresses and computational modeling of brazing process

Generation of residual stresses during the brazing process is inevitable. **The main cause of the generation of residual stresses is differential expansion and contraction of different materials during the non-uniform heating and cooling in brazing. Specifically, since the expansion of the braze alloy has been plastically compressed by WC and steel at temperature, on-cooling the braze will shrink to a smaller dimension, which generates a tensile stress in the braze joint**. Residual stresses during brazing process develop due to the differences in temperature distributions and coefficients of thermal expansion, which for

WC-Co, braze, and steel are shown in the Table 8. The cemented carbide is nearly 1/4 of the coefficient of thermal expansion (CTE) in comparison to the braze. The elastic modulus of the cemented carbide does not change significantly with temperature when compared to steel. It should also be noted that the yield strength of cemented carbide is much higher compared to steel and the braze. The variation in the thermophysical properties of the cemented carbide, steel, and braze materials results in the development of residual stresses during brazing.

Table 8. Elastic modulus, Coefficient of thermal expansion, Yield strength and Poisson's ratio of cemented carbide, steel and filler metal as a function of temperature [27].

Material	**Temperature (°C)**	**Elastic Modulus (GPa)**	**CTE**	**Yield Strength (MPa)**	**Poisson's ratio**
Cemented carbide	20	540	5.5	1500	0.28
	227	535	6.0	-	-
	427	530	6.9	-	-
	527	510	8.1	-	-
	800	500	9.0	-	-
Steel	20	10	210	235	0.285
	200	200	12.5	200	0.29
	600	150	14.5	125	0.315
	800	50	18	50	0.38
Cu-Zn-Mn	20	100	20.3	510	0.36

Finite element modeling (FEM) has been generally used for the estimation of residual stresses during brazing. Simulating the residual stresses requires accurate material properties (Table 8), especially at elevated temperatures, and the thermal profile experienced during brazing. Figure 19a shows a schematic of the geometry of WC-Co/braze/steel assembly used for the Finite element simulation. Numerical simulation of residual stresses in a cemented carbide/CuZn/steel braze has revealed the development of residual stresses near the seam in the cemented carbide [27]. These tensile stresses in cemented carbide eventually result in the fracture of the joint. Highest magnitude of the stress is close to the yield strength of the braze alloy used. The magnitude of residual stress was also found to increase with decreasing cooling temperature after brazing, with highest stresses at the room temperature. In order to reduce the residual stresses, some amount of external compressive stress is generally applied on the specimen during brazing [94]. Compressive stresses at high temperature deform the steel part because of its lowest yield strength among three materials. Plastic deformation of steel compensates its contraction during the cooling and hence reduces the mismatch in strain, thus also reducing the residual stress. Application of the external compressive stress on cemented carbide/CuZn/steel was found to result in lowering of residual stresses. Effect of external compressive load on the joint strength was also experimentally verified. In case of no external load, brazed joint was fractured through the cemented carbide. However, the shear strength of the brazed joint was 21% higher and fracture was along the interface in case of externally applied compressive load of 60 MPa [27].

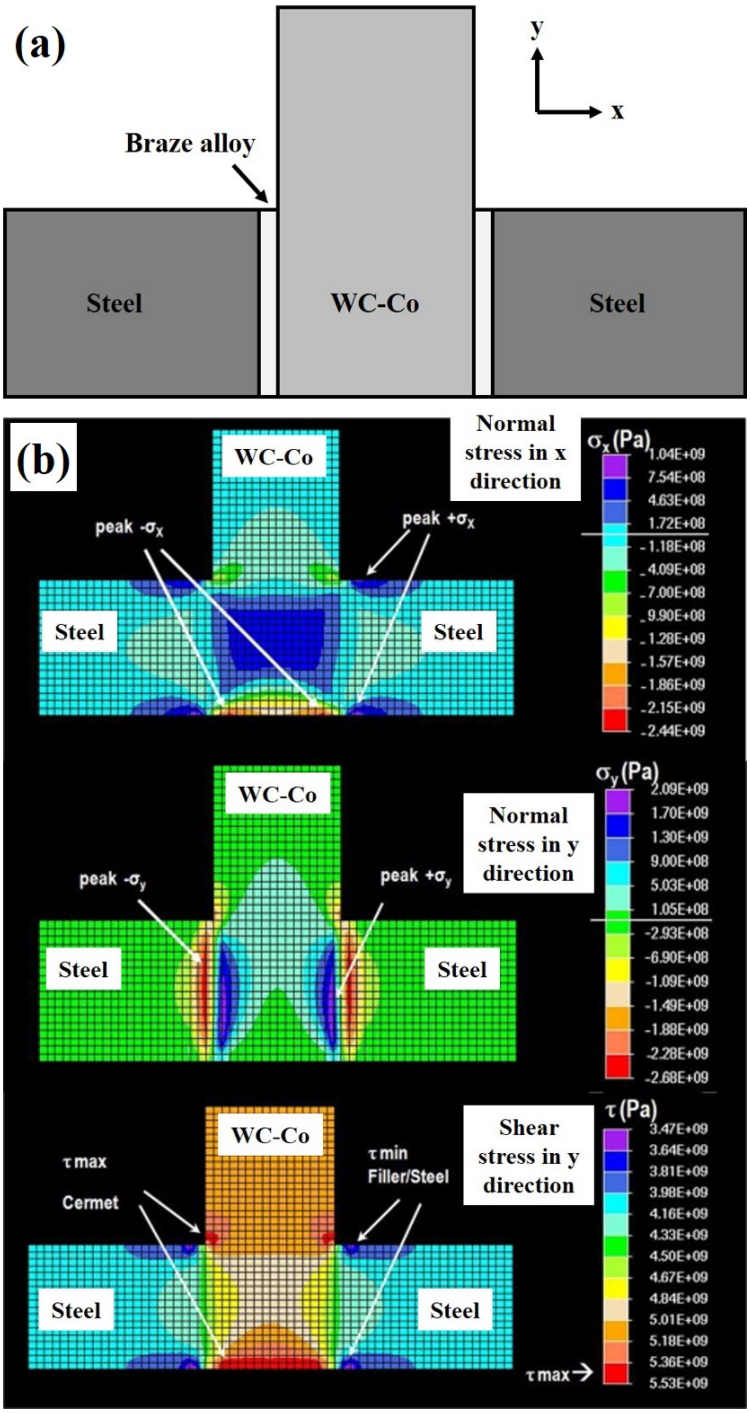

Figure 19. (a) Schematic of a two-dimensional finite element model, (b) Two-dimensional finite element stress distribution with associate mesh for simulating the residual stresses in a brazed cemented carbide-steel joint. The principal stress components (σ_x, σ_y) and the shear stress component (τ) is shown [26]

Figure 19b shows the 2-D finite element stress distribution in a different WC-Co/braze/steel system after brazing [26]. As shown in the figure, compressive residual stresses are developed in the cemented carbide, with a maximum value of

stress observed close to the interface between cemented carbide/braze/steel. As a result of the higher residual stresses, the cemented carbide close to the cemented carbide/braze/steel interface is the weakest and is prone to spallation. Simulations at various heating rates conclude that the optimization of heating rates during brazing is required. While a very high heating rate would result in higher residual stresses at the interlayer, thereby reducing the joint strength, a very low heating rate is going to result in excessive oxidation at the interlayer, which in turn results in poor wettability of the braze. Residual stresses were also found to decrease with the increase in brazing times. This was also experimentally verified by the shear strength values of joints brazed at different times. Higher shear strength, observed for the higher brazing times, established the reliability of the FEM simulations [26].

Although the locations for relatively higher and lower residual stresses are as expected, the magnitudes of the maximum stresses are higher than 1 GPa [26], which is unrealistic. Such stresses from FEM simulations indicate that authors considered the materials as linear elastic without considering plasticity. Hence, it is suggested to incorporate the plastic properties of the different materials in FEM simulations in order to obtain more realistic magnitudes of the residual stresses.

Generation of residual stresses during brazing of disimilar materials such as cemented carbides and steels presents challenges in achieving superior brazed joints. However, these challenges also present new opportunities for systematic investigations into the optimization of brazing process parameters for cemented carbides - steel system. These studies would be interesting avenues to mitigate the residual stresses. Specific challenges and recommendations are further discussed in a later section.

6. Discussion

The strength of the brazed joints depends on a number of factors which are either process dependent such as time and temperature of brazing or material dependent such as type of filler alloy used, composition of the cemented carbide, or dependent on both process and materials, such as generation of residual stresses. In order to improve the joint strength of WC-Co/Steel system, filling the gaps in the existing understanding of the brazing process and associated metallurgy is essential.

Optimizing process parameters **-** The main metallurgical changes associated with the increase in brazing temperature/time is the migration of Co from the cemented carbide towards the braze, and the migration of solutes, especially Cu, from the braze towards the WC-Co/braze interface. Such a migration either at prolonged time or at higher brazing temperature will result in one or more of the following metallurgical changes depending on the filler alloy chemistry, brazing temperature, and brazing time:

(1) Formation of intermetallic compounds at the interface of cemented carbide/filler alloy [30,37].
(2) Formation of Co depleted region at the interface of cemented carbide/filler alloy [50].
(3) Reduction in the fraction of solid solution phase in the braze [28,33,51].

These metallurgical changes at higher brazing temperature/time result in a de-

terioration of joint strength of the brazed joint (Figure 1). Brazing at lower temperature/time, on the other hand, also results in low joint strength due to inadequate wetting as a result of insufficient migration of elements. In order to overcome this challenge, some efforts have been made to vary the brazing temperature and time, and find out the optimized combination of time and temperature for brazing that provides adequate wetting and at the same time, does not lead to the formation of intermetallic compounds and solute depleted regions. Optimized brazing temperature - time resulted in an increase in the joint strength [28,33,34]. Although optimizing the time and temperature of brazing by varying these parameters results in increasing the strength of brazed joints, more research into the underlying mechanisms of the formation of solute depleted zone and intermetallic compounds is required to obtain superior joint strengths. In addition, a higher fraction of Cu solid solution is also expected to increase the strength of brazed joint. However, at a particular fraction of Cu solid solution, their distribution in the braze determines the extent of contribution to the joint strength. Depending on whether Cu solid solution phase is in the form of uniformly distributed island phase or as an isolated layer at the braze/base metal interface, its strengthening effect is going to be different [33].

An interesting parameter that needs thorough investigation is the thickness of filler metal. Thickness of filler, in combination with interdiffusion behavior of different alloying elements, especially Ni and Co in cemented carbide brazing systems, influences the brazed joint strength [37,87]. While research is being conducted to optimize the braze filler metal thickness to obtain stronger brazed joints, an initial thickness of about 0.004 inches as recommended by the American Welding Society (AWS) [59] can be a good starting point, from which optimization of the filler metal thickness for particular brazing process can be conducted. This thickness can result from a compromise between the high strengths associated with very thin joints (less than 150 microns) and the superior ability of thicker brazes (more than 150 microns) to absorb thermal and mechanical strains. Since the diffusion of different elements across the braze/base metal interfaces governs the formation of intermetallic compounds and solute depleted regions [37,50], understanding the interdiffusion behavior of alloying elements across the brazed joint is essential.

Filler alloy design and binder composition of cemented carbide - Apart from the alloying effects discussed in the earlier section (Section 3), further improvement of the commercially available BAg22 and BAg24 filler metals is the design of tri-metal brazes that include sandwiching Cu in between BAg22 and BAg24 layers. One specified thickness ratio of BAg22: Cu: BAg22 is 1:2:1. Sandwiching Cu in between the silver-based brazes minimizes the internal stresses in the joint because of the high ductility of Cu [79,80]. While tri-metal brazes are commercially available, limited information is available regarding their brazing metallurgy and microstructure evolution during brazing. Investigating the effect of sandwiching a Cu interlayer can prove beneficial in understanding the metallurgy, which can in turn improve the brazed strength of such filler metals.

Integrated Computational Materials Engineering (ICME) approach is suggested for filler metal design, especially for brazing WC-Co to steel. Use of computational thermodynamic tools such as ThermoCalc/DICTRA/PRISMA to develop filler alloys needs to be explored, which can accelerate the development of filler alloys

by reducing the number of experiments, and even generate new filler alloys that have not been explored. ICME approach would provide the information about solidus and liquidus temperatures, coefficient of thermal expansion, and type of phases present for a given composition of filler alloy. Conducting the survey for a range of compositions would provide temperature range, for example, for the formation of intermetallic compounds and hence also provide a better control over the expected microstructure at the joint. Material properties such as coefficient of thermal expansion would be useful as an input for FEM. To the best of the authors knowledge, no studies have been published, where ICME has been used to quantify the observed microstructure evolution during brazing and development of filler alloys. It is only recently that newly developed nickel based filler metal, high-entropy alloy, and amorphous fller metals were experimentally utilized in brazing of ceramics-metals and metals-metals [92,95,96]. Some of these alloys have been shown to decrease the formation of intermetallic compounds and hence increase the joint strength [93].

Lastly, there are two effects of WC binder composition on the joint strength. One is the addition of Cr_3C_2 to improve the joint strength of WC-Co/steel joints. While the increase in joint strength is attributed to an increase in the fraction of the η phase [30], a transition from Cr_3C_2 to Cr_7C_3 at higher brazing temperature/time may deteriorate the joint strength. Another effect is the change in the Co content in the cemented carbide. The joint strength increases initially with the increase in Co content, followed by a reduction in joint strength [41]. Hence, we suggest further investigation into the mechanism responsible for the reduction in joint strength at higher Co content. More studies are needed for establishing the role of Co migration and formation of a reaction layer at the braze/WC-Co interface in determining the change in joint strength [33].

Experimental verification of residual stresses - Residual stresses resulted from brazing of cemented carbides and steels affect the strength of brazed joints [26,27]. In order to decrease the residual stresses, functionally graded cemented carbide components were developed that can improve the wettability and reduce residual stresses [49]. Another method to reduce the internal stresses was adopted by applying an external stress on the brazed sample during the cooling cycle [27]. However, understanding the development of residual stresses, their measurement using experimental tools (e.g., X-ray diffraction, imaging with digital image correlation) would open doors to newer ways in overcoming this challenge. As discussed, the majority of the published research on modeling studies on brazing of WC-Co/steel joints focus on residual stresses developed during the brazing process. While modeling of the brazing phenomenon has been conducted in the literature [26,27], further research related to the evolution of residual stresses and their effect on the mechanical performance of the joint should be conducted on:

(1) Experimental verification of the developed residual stresses via XRD.
(2) In-situ monitoring of evolution of residual stresses during brazing using advanced characterization techniques, such as imaging with digital image correlation (DIC) and neutron diffraction. Data from these techniques can also feed into the development and refinement of the model.
(3) Modeling of damage mechanism during impact/shear loading. While majority of the published studies focus on the shear loading at low strain rates (usually at 0.5 mm/min - 2 mm/min), limited data is available on impact loading, which is more conducive to WC spallation phenomenon. Since the joint strength under

static loading is influenced by the brazing parameters and the underlying microstructural changes (Section 2), a similar trend in properties as a function of brazing parameters is expected under dynamic impact loading. Moreover, studying the impact performance of WC-Co/steel joints is crucial for resource based industries because of severe impact loading by rocks, sands, and clay [97].

7. Summary

(1) Factors influencing the joint strength of brazed joints of cemented carbide/steel joints have been reviewed. Braze joint strength is affected by a multitude of factors, the most important being brazing time and brazing temperature (controlled by current and voltage if using electric energy). A suitable optimization of these parameters is necessary to avoid the formation of intermetallics and depletion of Co at the interface. Future research into the understanding of strengthening effect, evolution of Cu solid solution, and interdiffusion of different alloying elements would provide essential knowledge about the metallurgical changes in and near the joint.
(2) Apart from the conventional BAg22 and BAg24 alloys, tri-metal brazes, Ni-based fillers, high-entropy alloys, and amorphous filler metals can be considered as potential filler metals to braze cemented carbides to steel. Use of computational tools such as ThermoCalc/DICTRA/PRISMA to develop filler alloys needs to be explored. This can accelerate the development of filler alloys by reducing the number of experiments, and even generate new filler alloy compositions.
(3) Future research along the directions of exploring the optimization of heating rates during brazing, in-situ monitoring of residual stresses using DIC, and developing new filler alloys to mitigate residual stresses, will prove beneficial to the brazing community at large. Controlling the binder composition, through the Ni/Co ratio and addition of Cr_3C_2 to the binder, significantly influences the microstructure and hence joint strength. Further research on detailed understanding behind the phase transitions at the brazed joint can prove beneficial in the commercialization of such novel binders.

Author Contributions

Writing–original draft preparation, N.K.S. and R.K.; Writing–review and editing, all authors; supervision, L.L. All authors have read and agreed to the published version of the manuscript.

Funding

The authors would like to acknowledge MITACS and Innotech Alberta, Canada for the funding through Elevate Program

Conflicts of Interest

The authors declare no conflict of interest.

References

[1] R. Armstrong, "The hardness and strength properties of WC-Co composites," *Materials*, vol. 4, no. 7, pp. 1287–1308, 2011.

[2] K. Plucknett, C. Jin, C. Onuoha, T. Stewart, and Z. Memarrashidi, "The Sliding Wear Response of High-Performance Cermets," in *Handbook of Mechanics of Materials*, pp. 1–42, Springer Singapore, 2018.

[3] J. Brezinová, M. Landová, A. Guzanová, L. Dulebová, and D. Draganovská, "Microstructure, wear behavior and corrosion resistance of WC-FeCrAl and WC-WB-Co coatings," *Metals*, vol. 8, no. 6, 2018.

[4] D. Jianxin, Z. Hui, W. Ze, L. Yunsong, and Z. Jun, "Friction and wear behaviors of WC/Co cemented carbide tool materials with different WC grain sizes at temperatures up to 600 °C," *International Journal of Refractory Metals and Hard Materials*, vol. 31, pp. 196–204, 2012.

[5] Q. Su, S. Zhu, H. Ding, Y. Bai, and P. Di, "Comparison of the wear behaviors of advanced and conventional cemented tungsten carbides," *International Journal of Refractory Metals and Hard Materials*, vol. 79, pp. 18–22, 2019.

[6] M. Jonke, T. Klünsner, P. Supancic, W. Harrer, J. Glätzle, R. Barbist, and R. Ebner, "Strength of WC-Co hard metals as a function of the effectively loaded volume," *International Journal of Refractory Metals and Hard Materials*, vol. 64, pp. 219–224, 2017.

[7] C. Liu, "Alternative binder phases for WC cemented carbides. *Master's thesis, KTH Royal Institute of Technology*," 2014.

[8] J. Tarragó, C. Ferrari, B. Reig, D. Coureaux, L. Schneider, and L. Llanes, "Mechanics and mechanisms of fatigue in a WC-Ni hardmetal and a comparative study with respect to WC-Co hardmetals," *International Journal of Fatigue*, vol. 70, pp. 252–257, 2015.

[9] J. Marshall and M. Giraudel, "The role of tungsten in the Co binder: Effects on WC grain size and hcp-fcc Co in the binder phase," *International Journal of Refractory Metals and Hard Materials*, vol. 49, no. 1, pp. 57–66, 2015.

[10] M. Tarraste, J. Kübarsepp, K. Juhani, A. Mere, M. Kolnes, M. Viljus, and B. Maaten, "Ferritic chromium steel as binder metal for WC cemented carbides," *International Journal of Refractory Metals and Hard Materials*, vol. 73, pp. 183–191, 2018.

[11] S. Sheikh, R. M'Saoubi, P. Flasar, M. Schwind, T. Persson, J. Yang, and L. Llanes, "Fracture toughness of cemented carbides: Testing method and microstructural effects," *International Journal of Refractory Metals and Hard Materials*, vol. 49, no. 1, pp. 153–160, 2015.

[12] S. Doi and M. Yasuoka, "Fracture toughness K_{IC} of cemented carbide WC-Co," *WIT Transactions on Engineering Sciences*, vol. 64, pp. 217–226, 2009.

[13] P. Jewell, L. Shannahan, S. Pagano, R. DeMott, M. Taheri, and L. Lamberson, "Rate and microstructure influence on the fracture behavior of cemented carbides WC-Co and WC-Ni," *International Journal of Fracture*, vol. 208, no. 1-2, pp. 203–219, 2017.

[14] B. Ma, X. Wang, C. Chen, D. Zhou, P. Xu, and X. Zhao, "Dissimilar welding and joining of cemented carbides," *Metals*, vol. 9, no. 11, p. 1161, 2019.

[15] W. Tillmann and N. Sievers, "Feasibility study of fluxless brazing cemented carbides to steel," in *IOP Conference Series: Materials Science and Engineering*, vol. 181, p. 012007, IOP Publishing, 2017.

[16] H. Ji, M. Li, Y. Lu, and C. Wang, "Mechanical properties and microstructures of hybrid ultrasonic resistance brazing of WC-Co/BeCu," *Journal of Materials Processing Technology*, vol. 212, no. 9, pp. 1885–1891, 2012.

[17] A. Laansoo, J. Kübarsepp, V. Vainola, and M. Viljus, "Induction brazing of cermets to steel," *Estonian Journal of Engineering*, vol. 18, no. 3, p. 232, 2012.

[18] T. Iamboliev, S. Valkanov, and S. Atanasova, "Microstructure embrittlement of hard metal-steel joint obtained under induction heating diffusion bonding," *International Journal of Refractory Metals and Hard Materials*, vol. 37, pp. 90–97, 2013.

[19] M. Barrena, J. de Salazar, and L. Matesanz, "Ni-Cu alloy for diffusion bonding cer-

met/steel in air," *Materials Letters*, vol. 63, no. 24-25, pp. 2142–2145, 2009.
[20] K. Feng, H. Chen, J. Xiong, and Z. Guo, "Investigation on diffusion bonding of functionally graded WC-Co/Ni composite and stainless steel," *Materials and Design*, vol. 46, pp. 622–626, 2013.
[21] P. Xu, J. Ren, P. Zhang, H. Gong, and S. Yang, "Analysis of formation and interfacial WC dissolution behavior of WC-Co/Invar laser-TIG welded joints," *Journal of Materials Engineering and Performance*, vol. 22, no. 2, pp. 613–623, 2013.
[22] D. Zhou, H. Cui, P. Xu, and F. Lu, "Tungsten Carbide Grain Size Computation for WC-Co Dissimilar Welds," *Journal of Materials Engineering and Performance*, vol. 25, no. 6, pp. 2500–2510, 2016.
[23] C. Barbatti, J. Garcia, G. Liedl, and A. Pyzalla, "Joining of cemented carbides to steel by laser beam welding," *Materialwissenschaft und Werkstofftechnik*, vol. 38, no. 11, pp. 907–914, 2007.
[24] Z. Mirski, K. Granat, and S. Stano, "Possibilities of laser-beam joining cemented carbides to steel," *Welding International*, vol. 30, no. 3, pp. 187–191, 2016.
[25] P. Xu, D. Zhou, and L. Li, "Fiber laser welding of WC-Co and carbon steel dissimilar materials," *Welding Journal*, vol. 96, no. 1, pp. 1s–10s, 2017.
[26] M. Barrena, J. De Salazar, and M. Gómez-Vacas, "Numerical simulation and experimental analysis of vacuum brazing for steel/cermet," *Ceramics International*, vol. 40, no. 7 Part B, pp. 10557–10563, 2014.
[27] J. Zhang and L. Jin, "Numerical simulation of residual stress in brazing joint between cemented carbide and steel," *Materials Science and Technology*, vol. 21, no. 12, pp. 1455–1459, 2005.
[28] B. Cheniti, D. Miroud, R. Badji, D. Allou, T. Csanádi, M. Fides, and P. Hvizdoš, "Effect of brazing current on microstructure and mechanical behavior of WC-Co/AISI 1020 steel TIG brazed joint," *International Journal of Refractory Metals and Hard Materials*, vol. 64, pp. 210–218, 2017.
[29] X. Zhang, G. Liu, J. Tao, Y. Guo, J. Wang, and G. Qiao, "Brazing of WC–8Co cemented carbide to steel using Cu–Ni–Al alloys as filler metal: Microstructures and joint mechanical behavior," *Journal of Materials Science and Technology*, vol. 34, no. 7, pp. 1180–1188, 2018.
[30] W. Lee, B. Kwon, and S. Jung, "Effects of Cr_3C_2 on the microstructure and mechanical properties of the brazed joints between WC-Co and carbon steel," *International Journal of Refractory Metals and Hard Materials*, vol. 24, no. 3, pp. 215–221, 2006.
[31] H. Chen, K. Feng, S. Wei, J. Xiong, Z. Guo, and H. Wang, "Microstructure and properties of WC-Co/3Cr13 joints brazed using Ni electroplated interlayer," *International Journal of Refractory Metals and Hard Materials*, vol. 33, pp. 70–74, 2012.
[32] M. Uzkut, N. Köksal, and B. Ünlü, "The determination of element diffusion in connecting SAE 1040/WC material by brazing," *Journal of Materials Processing Technology*, vol. 169, no. 3, pp. 409–413, 2005.
[33] C. Jiang, H. Chen, Q. Wang, and Y. Li, "Effect of brazing temperature and holding time on joint properties of induction brazed WC-Co/carbon steel using Ag-based alloy," *Journal of Materials Processing Technology*, vol. 229, pp. 562–569, 2016.
[34] C. Jiang, H. Chen, X. Zhao, S. Qiu, D. Han, and G. Gou, "Microstructure and mechanical properties of brazing bonded WC-15Co/35CrMo joint using AgNi/CuZn/AgNi composite interlayers," *International Journal of Refractory Metals and Hard Materials*, vol. 70, pp. 1–8, 2018.
[35] L. Yajiang, Z. Zengda, H. Xiao, F. Tao, and W. Xinghong, "A study on microstructure in the brazing interface of WC–TiC–Co hard alloys," *International Journal of Refractory Metals and Hard Materials*, vol. 20, no. 3, pp. 169–173, 2002.
[36] Y. Li, Z. Zou, T. Feng, and X. Wang, "Oxidation resistance and phase constituents in the brazing interface of WC-TiC-Co hard alloys," *Journal of Materials Processing Technology*, vol. 122, no. 1, pp. 51–55, 2002.
[37] M. Hasanabadi, A. Shamsipur, H. Sani, H. Omidvar, and S. Sakhaei, "Interfacial mi-

crostructure and mechanical properties of tungsten carbide brazed joints using Ag-Cu-Zn + Ni/Mn filler alloy," *Transactions of Nonferrous Metals Society of China (English Edition)*, vol. 27, no. 12, pp. 2638–2646, 2017.

[38] S. Yaoita, T. Watanabe, and T. Sasaki, "Effects of Ni and Co elements in filler metals in Ag-brazing of cemented carbide," *Quarterly Journal of the Japan Welding Society*, vol. 30, no. 4, pp. 298–305, 2012.

[39] S. Yaoita, T. Watanabe, and T. Sasaki, "Effects of Ni and Co elements in filler metals in Ag brazing of cemented carbide," *Materials Research Innovations*, vol. 17, no. sup2, pp. s142–s147, 2013.

[40] K. Kaiwa, S. Yaoita, T. Sasaki, and T. Watanabe, "Effects of Ni and Co additions to filler metals on Ag-brazed joints of cemented carbide and martensitic stainless steel," in *Advanced Materials Research*, vol. 922, pp. 322–327, Trans Tech Publ, 2014.

[41] W. Lee, B. Kwon, and S. Jung, "Effect of bonding time on joint properties of vacuum brazed WC – Co hard metal/carbon steel using stacked Cu and Ni alloy as insert metal," *Materials Science and Technology*, vol. 20, no. 11, pp. 1474–1478, 2004.

[42] Y. Sui, H. Luo, Y. Lv, F. Wei, J. Qi, Y. He, Q. Meng, and Z. Sun, "Influence of brazing technology on the microstructure and properties of Yg20C cemented carbide and 16Mn steel joints," *Welding in the World*, vol. 60, no. 6, pp. 1269–1275, 2016.

[43] X. Zhang, G. Liu, J. Tao, H. Shao, H. Fu, T. Pan, and G. Qiao, "Vacuum brazing of WC-8Co cemented carbides to carbon steel using pure Cu and Ag-28Cu as filler metal," *Journal of Materials Engineering and Performance*, vol. 26, no. 2, pp. 488–494, 2017.

[44] A. Pieczara, T. Piotrowski, W. Leśniewski, M. Wawrylak, and P. Wieliczko, "The impact of brazing parameters on the strength of a WC/Co-filler metal-steel joint," *Journal of Machine Construction and Maintenance - Problemy Eksploatacji*, no. 3, pp. 59–64, 2015.

[45] N. Cole, R. Gilliland, and G. Slaughter, "Weldability of tungsten and its alloys," *Welding Journal*, vol. 50, no. 9, pp. 419–s, 1971.

[46] M. Amelzadeh and S. Mirsalehi, "Influence of braze type on microstructure and mechanical behavior of WC-Co/steel dissimilar joints," *Journal of Manufacturing Processes*, vol. 36, pp. 450–458, 2018.

[47] R. Gilliland and C. Adams, "Improved brazing methods for tungsten carbide tool bits," *Welding Journal*, vol. 50, no. 7, p. 267, 1971.

[48] I. Voiculescu, V. Geanta, H. Binchiciu, D. Iovanas, and R. Stefanoiu, "Dissimilar brazed joints between steel and tungsten carbide," in *IOP Conference Series: Materials Science and Engineering*, vol. 209, p. 012021, IOP Publishing, 2017.

[49] H. Chen, K. Feng, J. Xiong, and Z. Guo, "Characterization and stress relaxation of the functionally graded WC–Co/Ni component/stainless steel joint," *Journal of alloys and compounds*, vol. 557, pp. 18–22, 2013.

[50] L. Chiu, H. Wang, C. Huang, C. Hsu, and T. Chen, "Effect of brazing temperature on the microstructure and property of vacuum brazed WC-Co and carbon steel joint," in *Advanced materials research*, vol. 47, pp. 682–685, Trans Tech Publ, 2008.

[51] S. Mousavi, P. Sherafati, and M. Hoseinion, "Investigation on wettability and metallurgical and mechanical properties of cemented carbide and steel brazed joint," in *Advanced Materials Research*, vol. 445, pp. 759–764, Trans Tech Publ, 2012.

[52] P. Xu, "Dissimilar welding of WC–Co cemented carbide to $Ni_{42}Fe_{50.9}C_{0.6}Mn_{3.5}Nb_3$ Invar alloy by laser–tungsten inert gas hybrid welding," *Materials and Design*, vol. 32, no. 1, pp. 229–237, 2011.

[53] X. Peiquan, Z. Xiujuan, Y. Dexin, and Y. Shun, "Study on filler metal (Ni-Fe-C) during GTAW of WC-30Co to 45 inch carbon steel," *Journal of materials science*, vol. 40, no. 24, pp. 6559–6564, 2005.

[54] M. Barrena, J. De Salazar, and L. Matesanz, "Interfacial microstructure and mechanical strength of WC–Co/90MnCrV8 cold work tool steel diffusion bonded joint with Cu/Ni electroplated interlayer," *Materials and Design*, vol. 31, no. 7, pp. 3389–3394, 2010.

[55] R. Tashi, S. Mousavi, and M. Atabaki, "Diffusion brazing of Ti–6Al–4V and austenitic stainless steel using silver-based interlayer," *Materials and Design (1980-2015)*, vol. 54,

pp. 161–167, 2014.
[56] T. Yoshida and H. Ohmura, "Dissolution and deposit of base metal in dissimilar carbon steel brazing," *Welding journal*, vol. 59, no. 10, pp. 278–282, 1980.
[57] I. Azcona, A. Ordonez, J. Sanchez, and F. Castro, "Hot isostatic pressing of ultrafine tungsten carbide-cobalt hardmetals," *Journal of materials science*, vol. 37, no. 19, pp. 4189–4195, 2002.
[58] R. Edwards, "Joint tolerances in capillary copper piping joints," *Weld. J.*, vol. 6, pp. 321–324, 1972.
[59] AWS Committee on Brazing and Soldering, *Brazing Handbook*. American Welding Society, 1991.
[60] R. Rosen and M. Kassner, "Mechanical properties of soft-interlayer solid-state welds," *ASM International, ASM Handbook.*, vol. 6, pp. 165–172, 1993.
[61] J. Willingham, "Filler metals and fluxes for brazing tungsten carbide," *Johnson Matthey Metal Joining brochure*, 2008.
[62] M. Way, J. Willingham, and R. Goodall, "Brazing filler metals," *International Materials Reviews*, pp. 1–29, 2019.
[63] J. Kim, J. Hardy, and K. Weil, "Silver-copper oxide based reactive air braze for joining yttria-stabilized zirconia," *Journal of materials research*, vol. 20, no. 3, pp. 636–643, 2005.
[64] L. Zang, Z. Yuan, Z. Cao, H. Matsuura, and F. Tsukihashi, "Reactive wetting processes and triple-line configuration of Sn-3.5Ag on Cu substrates at elevated temperatures," *Journal of electronic materials*, vol. 41, no. 8, pp. 2051–2056, 2012.
[65] H. Chen, L. Li, R. Kemps, B. Michielsen, M. Jacobs, F. Snijkers, and V. Middelkoop, "Reactive air brazing for sealing mixed ionic electronic conducting hollow fibre membranes," *Acta Materialia*, vol. 88, pp. 74–82, 2015.
[66] X. Yue, P. He, J. Feng, J. Zhang, and F. Zhu, "Microstructure and interfacial reactions of vacuum brazing titanium alloy to stainless steel using an AgCuTi filler metal," *Materials Characterization*, vol. 59, no. 12, pp. 1721–1727, 2008.
[67] H. Li, H. Peng, T. Lin, P. Feng, J. Feng, and Y. Huang, "Microstructure and shear strength of reactive brazing joints of TiAl/Ni-based alloy," *Transactions of Nonferrous Metals Society of China*, vol. 22, no. 2, pp. 324–329, 2012.
[68] R. Shiue, S. Wu, and J. Shiue, "Infrared brazing of Ti–6Al–4V and 17-4 PH stainless steel with (Ni)/Cr barrier layer (s)," *Materials Science and Engineering: A*, vol. 488, no. 1-2, pp. 186–194, 2008.
[69] J. Kang, X. Song, S. Hu, D. Liu, W. Guo, W. Fu, and J. Cao, "Wetting and brazing of alumina by $Sn_{0.3}Ag_{0.7}$Cu-Ti alloy," *Metallurgical and Materials Transactions A*, vol. 48, no. 12, pp. 5870–5878, 2017.
[70] Z. Chen, H. Bian, C. Niu, X. Song, Y. Lei, C. Jin, J. Cao, and J. Feng, "Wetting and brazing of chromium film-deposited alumina using AgCu filler metal," *Journal of Materials Engineering and Performance*, vol. 27, no. 10, pp. 5470–5477, 2018.
[71] H. He, C. Wu, Z. Xie, Y. Liu, W. Xu, and Y. Jing, "Effects of alloyed fluxes on spreading behavior and microstructures of aluminum–titanium TIG brazing interface," *Metallography, Microstructure, and Analysis*, vol. 6, no. 1, pp. 82–88, 2017.
[72] Z. Zhang, B. Xiao, D. Duan, B. Wang, and S. Liu, "Investigation on the brazing mechanism and machining performance of diamond wire saw based on Cu-Sn-Ti alloy," *International Journal of Refractory Metals and Hard Materials*, vol. 66, pp. 211–219, 2017.
[73] O. Kozlova, M. Braccini, R. Voytovych, N. Eustathopoulos, P. Martinetti, and M. F. Devismes, "Brazing copper to alumina using reactive CuAgTi alloys," *Acta Materialia*, vol. 58, no. 4, pp. 1252–1260, 2010.
[74] H. Wang, J. Cao, and J. Feng, "Brazing mechanism and infiltration strengthening of CC composites to TiAl alloys joint," *Scripta Materialia*, vol. 63, no. 8, pp. 859–862, 2010.
[75] Y. Zhou, D. Liu, H. Niu, X. Song, X. Yang, and J. Feng, "Vacuum brazing of C/C composite to TC4 alloy using nano-Al2O3 strengthened AgCuTi composite filler," *Materials and Design*, vol. 93, pp. 347–356, 2016.
[76] Y. Zhao, M. Wang, J. Cao, X. Song, D. Tang, and J. Feng, "Brazing TC4 alloy to Si_3N_4 ce-

ramic using nano-Si_3N_4 reinforced AgCu composite filler," *Materials and Design*, vol. 76, pp. 40–46, 2015.
[77] Y. He, J. Zhang, P. Lv, and C. Liu, "Characterization of the Si_3N_4/42CrMo joints vacuum brazed with Pd modified filler alloy for high temperature application," *Vacuum*, vol. 109, pp. 86–93, 2014.
[78] S. Schittny, "Liquidus surface of the system Ag-Cu-Zn, *MSI, Materials Science International Services GmbH, Stuttgart*," 1988.
[79] "Silverbraze and trimetal 49Ni4 (BAg-22)," tech. rep., The Prince and Izant Company, 2020.
[80] "Silverbraze and trimetal 50Ni2 (BAg-24)," tech. rep., The Prince and Izant Company, 2020.
[81] G. Triantafyllou and J. Irvine, "Wetting and interactions of Ag–Cu–Ti and Ag–Cu–Ni alloys with ceramic and steel substrates for use as sealing materials in a DCFC stack," *Journal of Materials Science*, vol. 51, no. 4, pp. 1766–1778, 2016.
[82] L. Pan, J. Gu, W. Zou, T. Qiu, H. Zhang, and J. Yang, "Brazing joining of Ti_3AlC_2 ceramic and 40Cr steel based on Ag-Cu-Ti filler metal," *Journal of Materials Processing Technology*, vol. 251, pp. 181–187, 2018.
[83] Y. Li, Z. Zhu, Y. He, H. Chen, C. Jiang, D. Han, and J. Li, "Wc particulate reinforced joint by ultrasonic-associated brazing of WC-Co/35CrMo," *Journal of Materials Processing Technology*, vol. 238, pp. 15–21, 2016.
[84] T. Yamaguchi, K. Harano, and K. Yajima, "Spreading and reactions of molten metals on and with cemented carbides," in *Surfaces and interfaces in ceramic and ceramic—metal systems*, pp. 503–511, Springer, 1981.
[85] N. Ray, L. Froyen, K. Vanmeensel, and J. Vleugels, "Wetting and solidification of silver alloys in the presence of tungsten carbide," *Acta Materialia*, vol. 144, pp. 459–469, 2018.
[86] A. Amirnasiri, N. Parvin, and M. Haghshenas, "Dissimilar diffusion brazing of WC-Co to AISI 4145 steel using RBCuZn-D interlayer," *Journal of Manufacturing Processes*, vol. 28, pp. 82–93, 2017.
[87] J. Li, G. Sheng, and L. Huang, "Additional active metal Nb in Cu-Ni system filler metal for brazing of TiC cermet/steel," *Materials Letters*, vol. 156, pp. 10–13, 2015.
[88] A. Laansoo, J. Kübarsepp, and V. Vainola, "Brazing of TiC Cermet to Steel," in *7th International DAAAM Baltic Conference*, vol. 9, pp. 1–5, 2010.
[89] A. Laansoo, J. Kübarsepp, V. Vainola, and M. Viljus, "Induction brazing of cermets to steel," *Estonian Journal of Engineering*, vol. 18, no. 3, pp. 232–242, 2012.
[90] M. Singh and R. Asthana, "Joining of zirconium diboride-based ultra high-temperature ceramic composites using metallic glass interlayers," *Materials Science and Engineering: A*, vol. 460, pp. 153–162, 2007.
[91] M. Singh, R. Asthana, and T. Shpargel, "Brazing of ceramic-matrix composites to ti and hastealloy using ni-base metallic glass interlayers," *Materials Science and Engineering: A*, vol. 498, no. 1-2, pp. 19–30, 2008.
[92] Y. Liu, G. Wang, W. Cao, H. Xu, Z. Huang, D. Zhu, and C. Tan, "Brazing ZrB_2-SiC ceramics to Ti_6Al_4V alloy with TiCu-based amorphous filler," *Journal of Manufacturing Processes*, vol. 30, pp. 516–522, 2017.
[93] J. Zou, Z. Jiang, Q. Zhao, and Z. Chen, "Brazing of Si_3N_4 with amorphous $Ti_{40}Zr_{25}Ni_{15}Cu_{20}$ filler," *Materials Science and Engineering: A*, vol. 507, no. 1-2, pp. 155–160, 2009.
[94] J. Schijve, *Fatigue of structures and materials*. Springer Science & Business Media, 2001.
[95] D. Bridges, S. Zhang, S. Lang, M. Gao, Z. Yu, Z. Feng, and A. Hu, "Laser brazing of a nickel-based superalloy using a Ni-Mn-Fe-Co-Cu high entropy alloy filler metal," *Materials Letters*, vol. 215, pp. 11–14, 2018.
[96] Y. Xia, H. Dong, R. Zhang, Y. Wang, X. Hao, P. Li, and C. Dong, "Interfacial microstructure and shear strength of Ti_6Al_4V alloy/316L stainless steel joint brazed with $Ti_{33.3}Zr_{16.7}Cu_{50-x}Ni_x$ amorphous filler metals," *Materials and Design*, vol. 187, p. 108380, 2020.

[97] T. Joseph, "Physical, static and inferred dynamic loaded properties of oil sand, final progress report, phases I, II, and III, caterpillar," *Inc., Peoria, Illinois*, 2005.

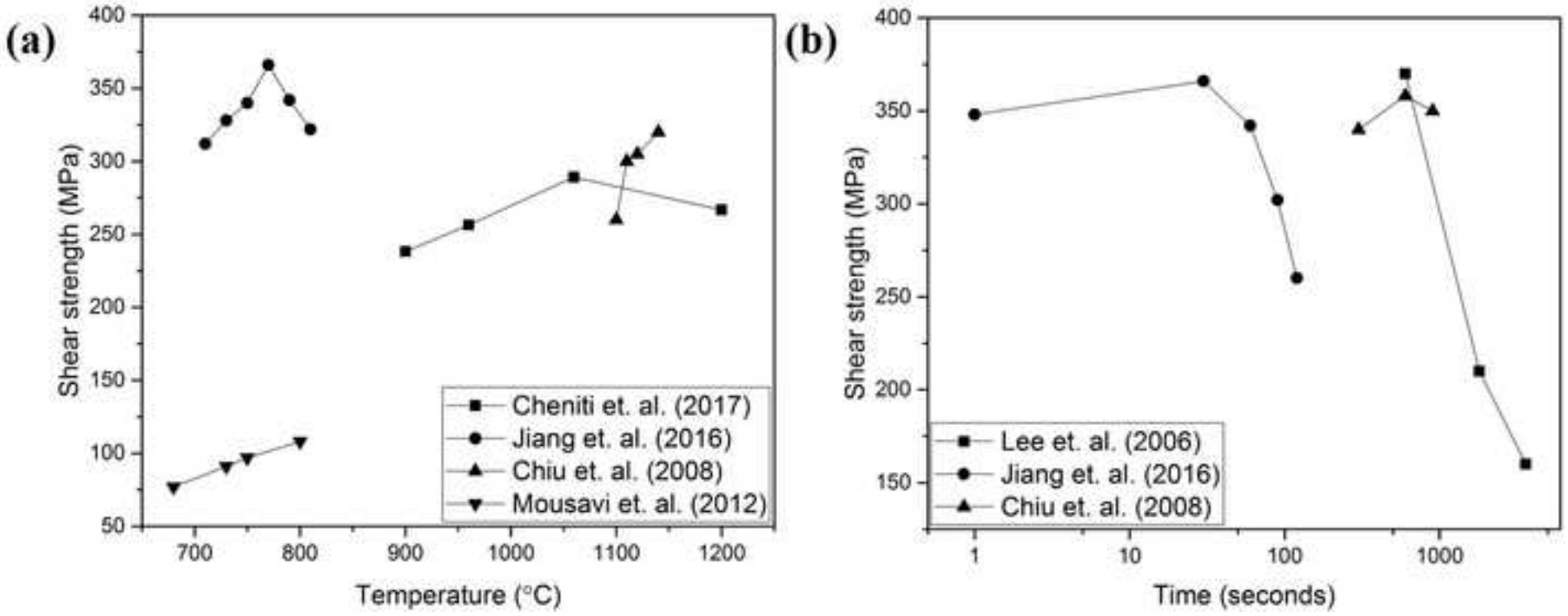

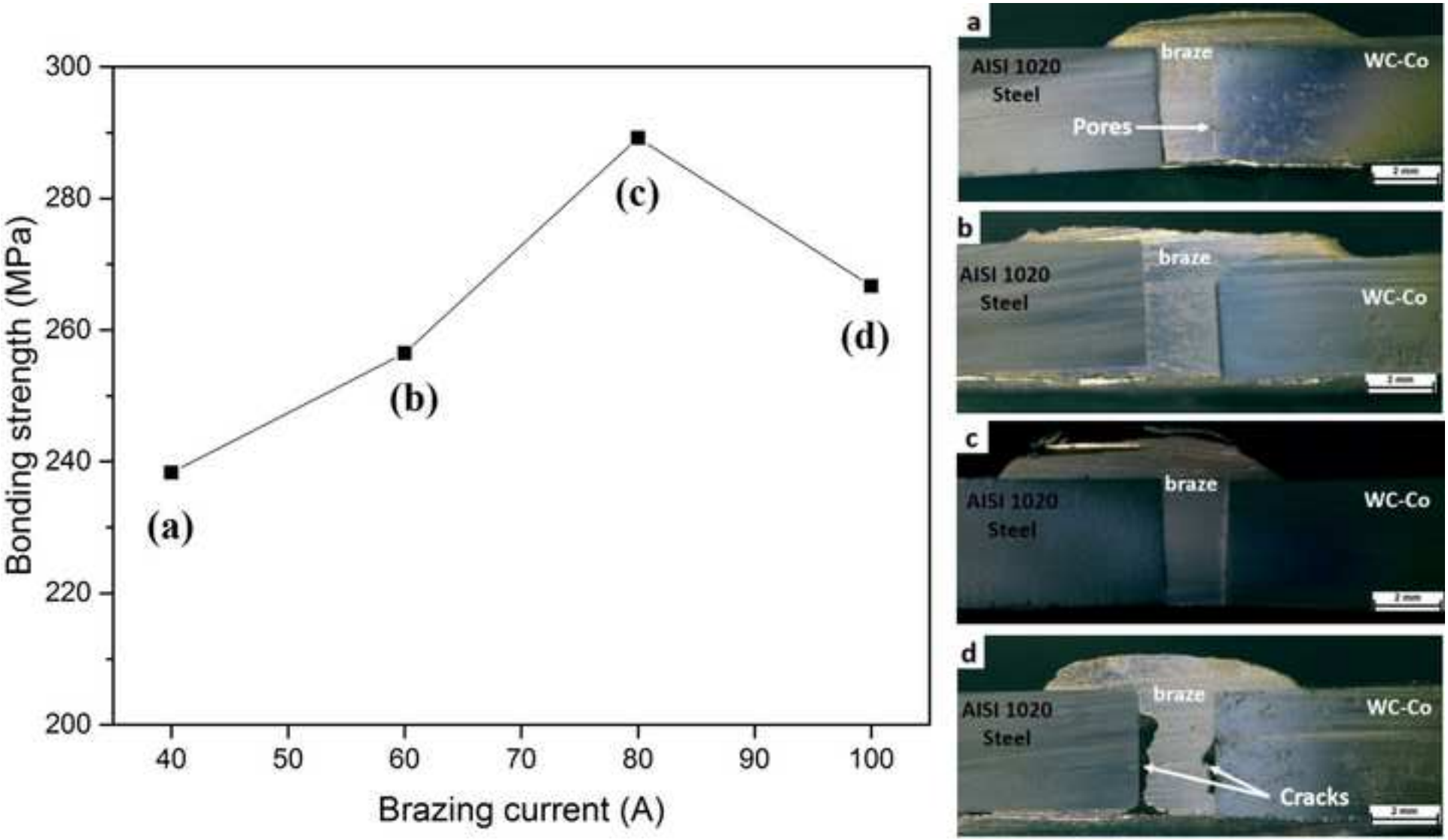

Colour figure

Click here to access/download;Colour figure;Fig 3.jpg

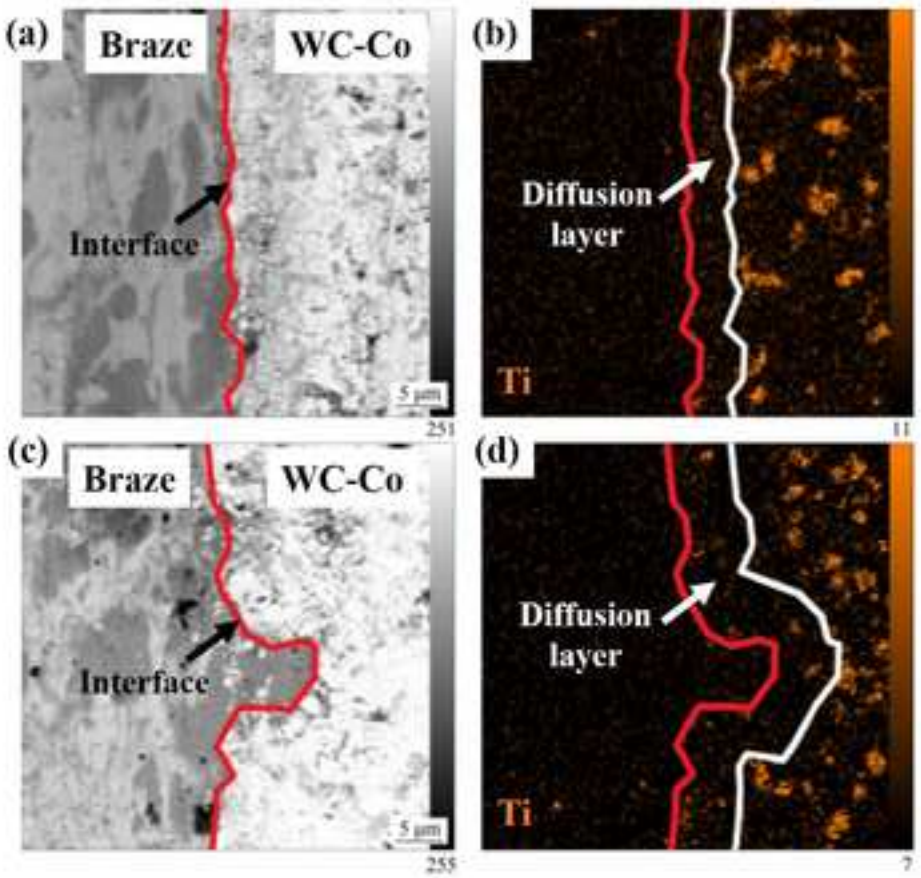

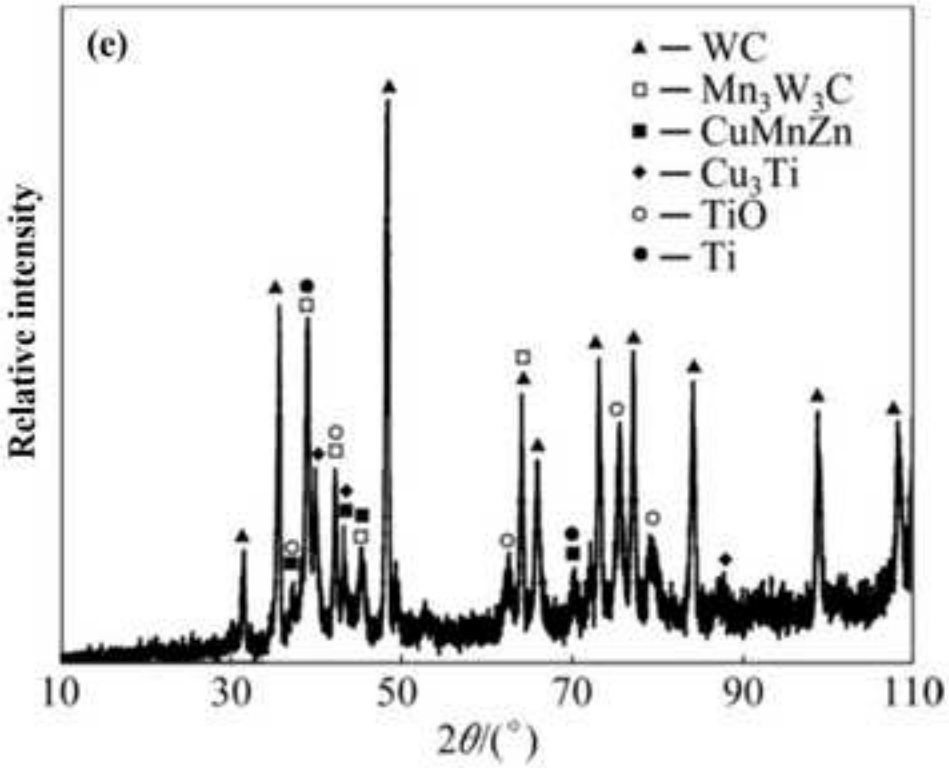

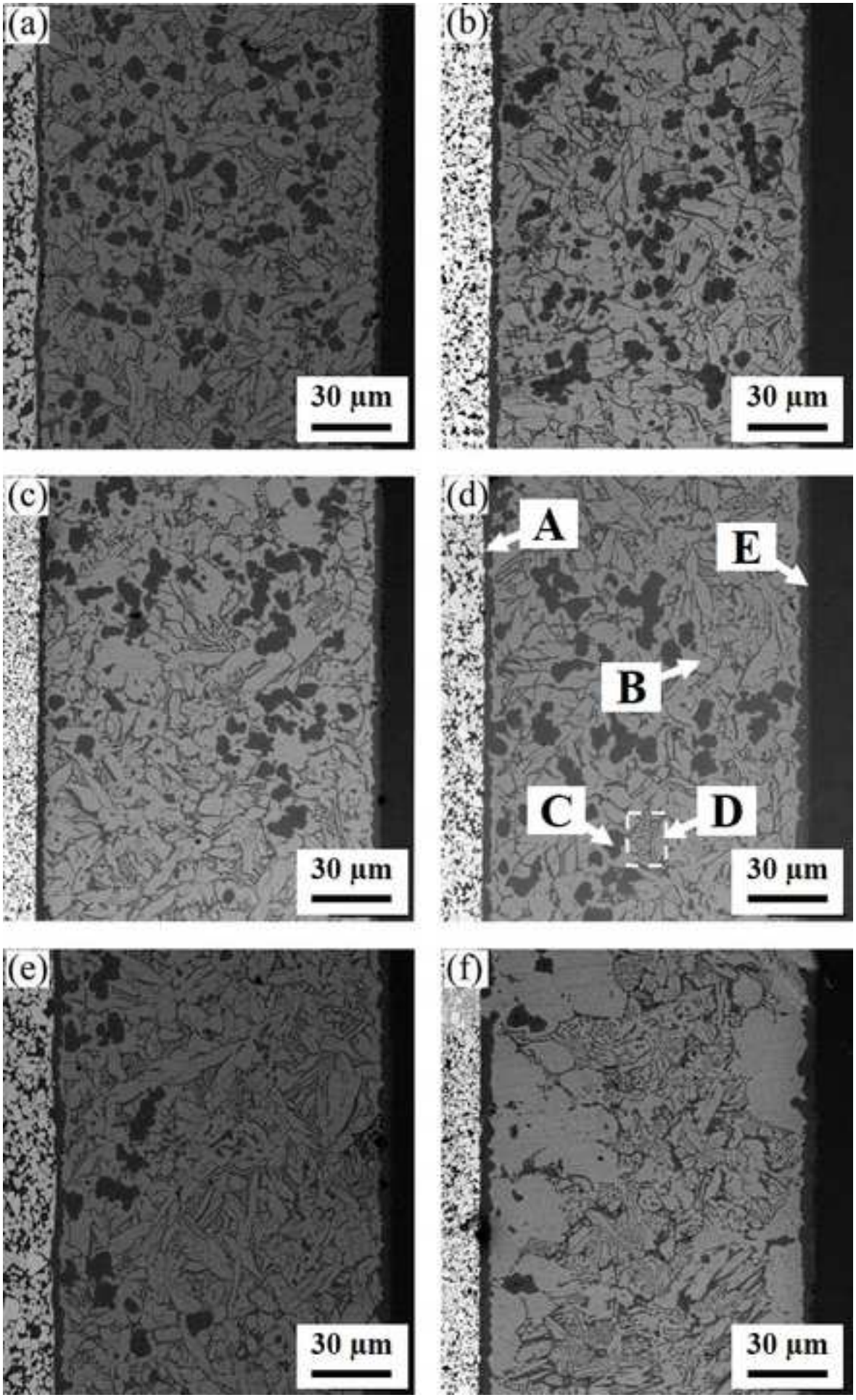

Colour figure

Click here to access/download;Colour figure;Fig 5.jpg

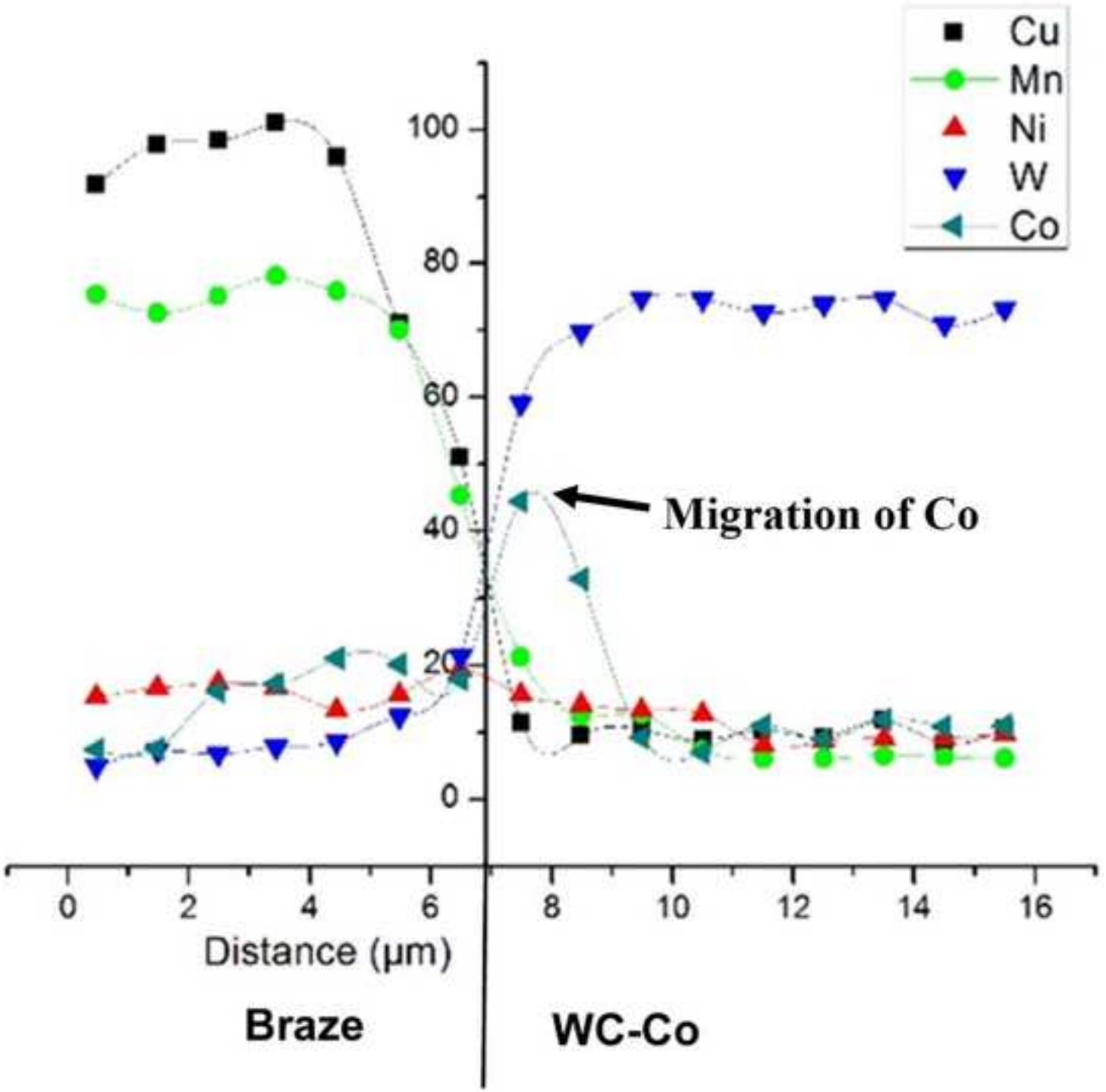

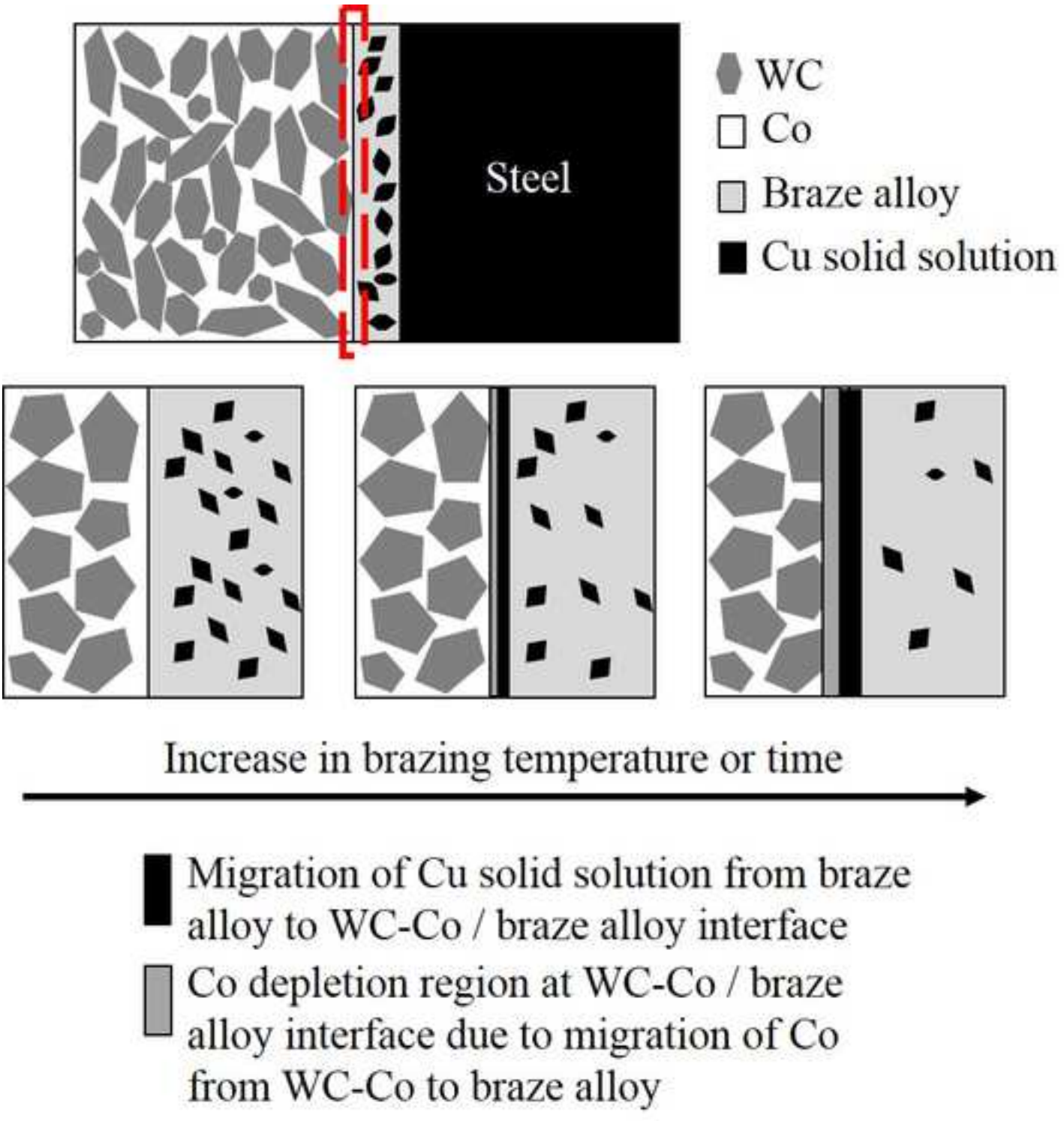

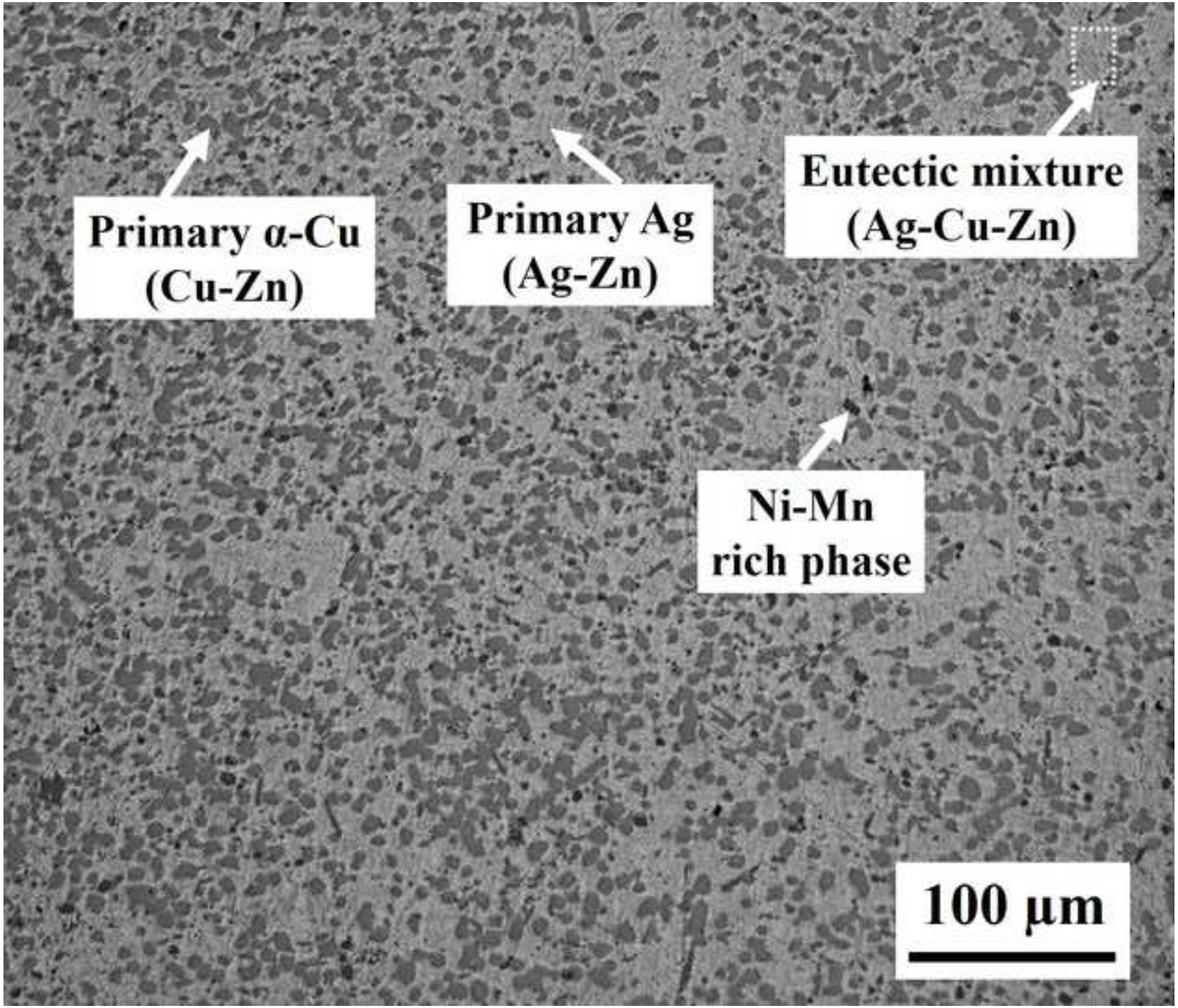

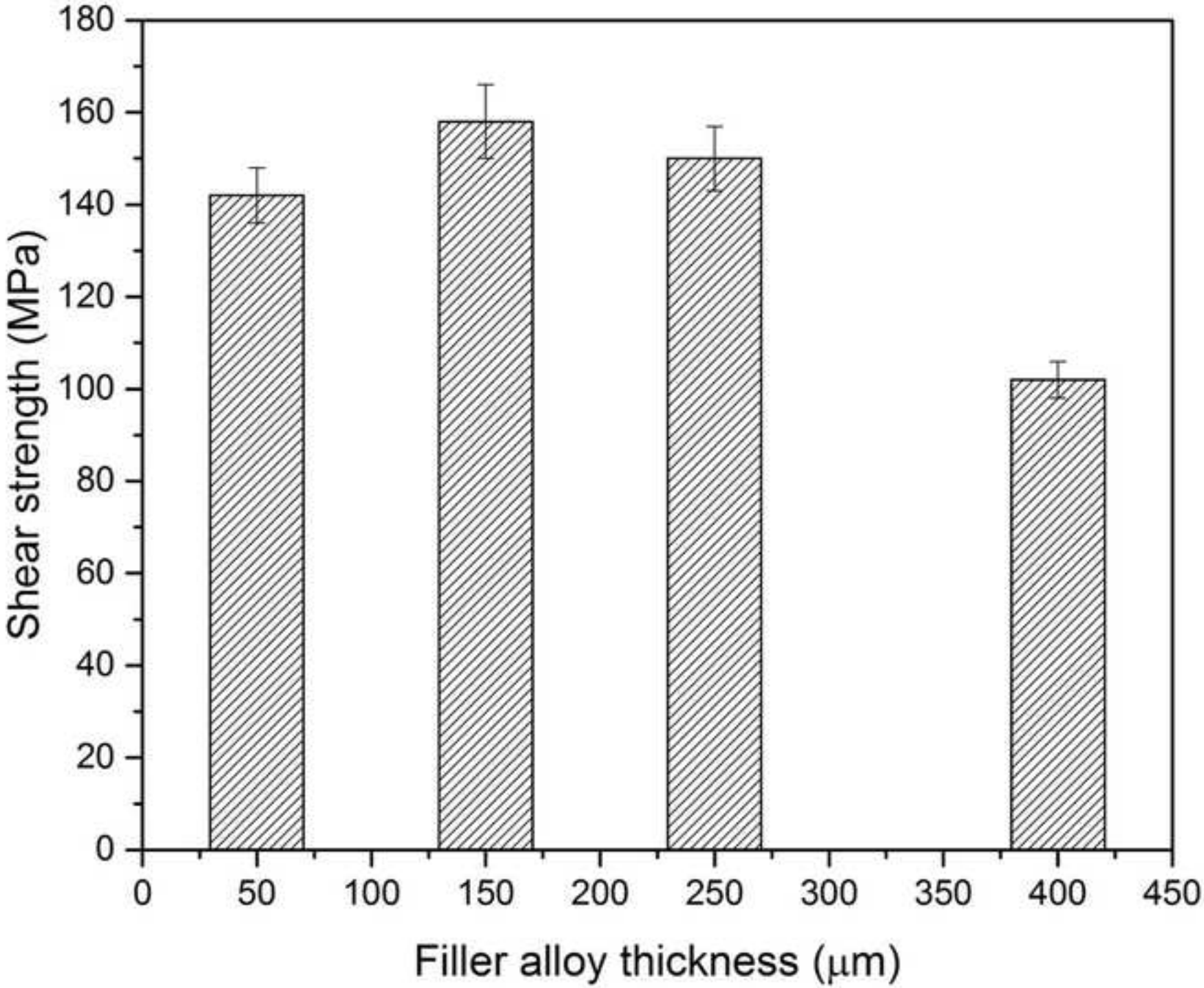

Colour figure

Click here to access/download;Colour figure;Fig 13.jpg

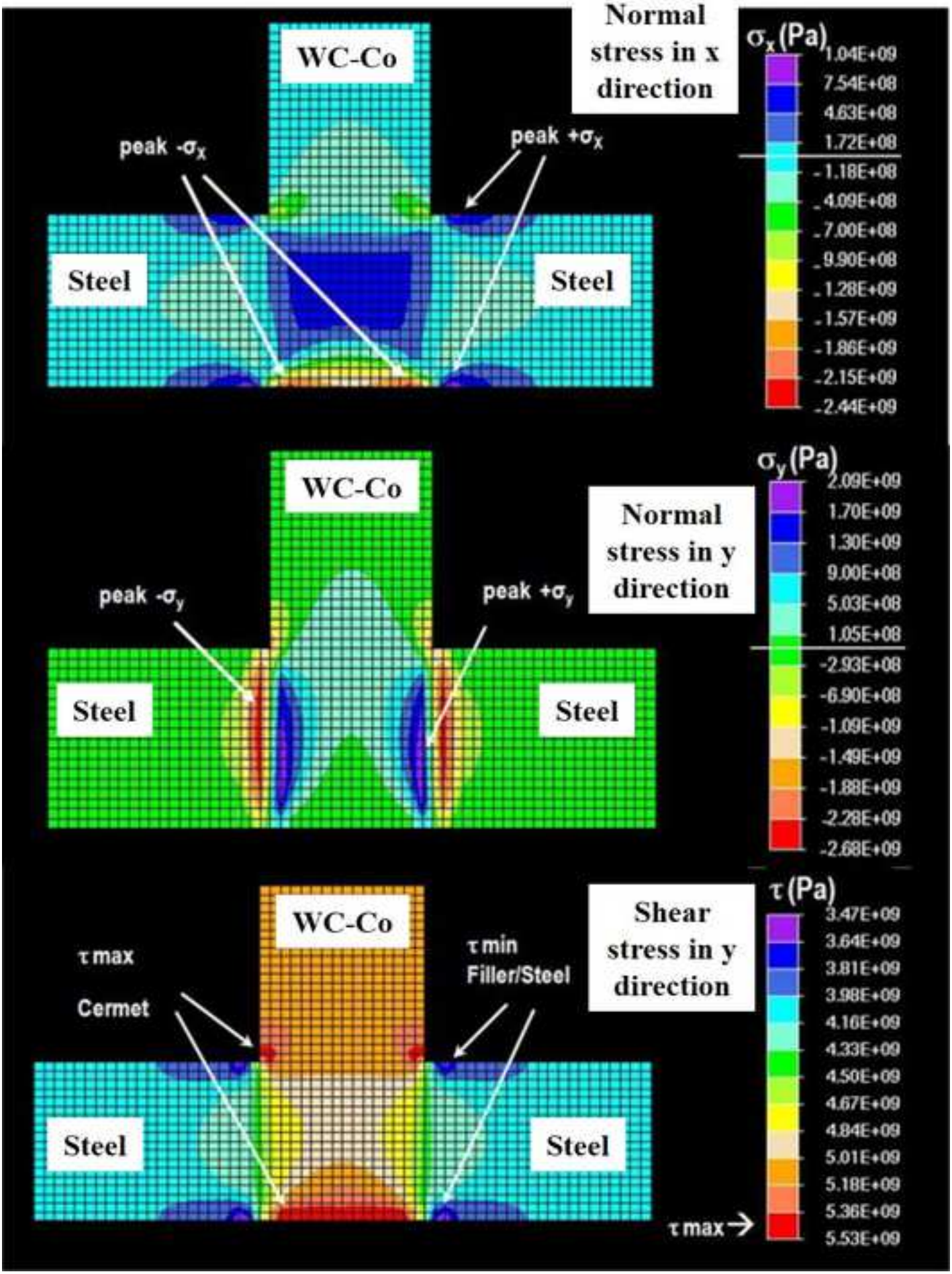

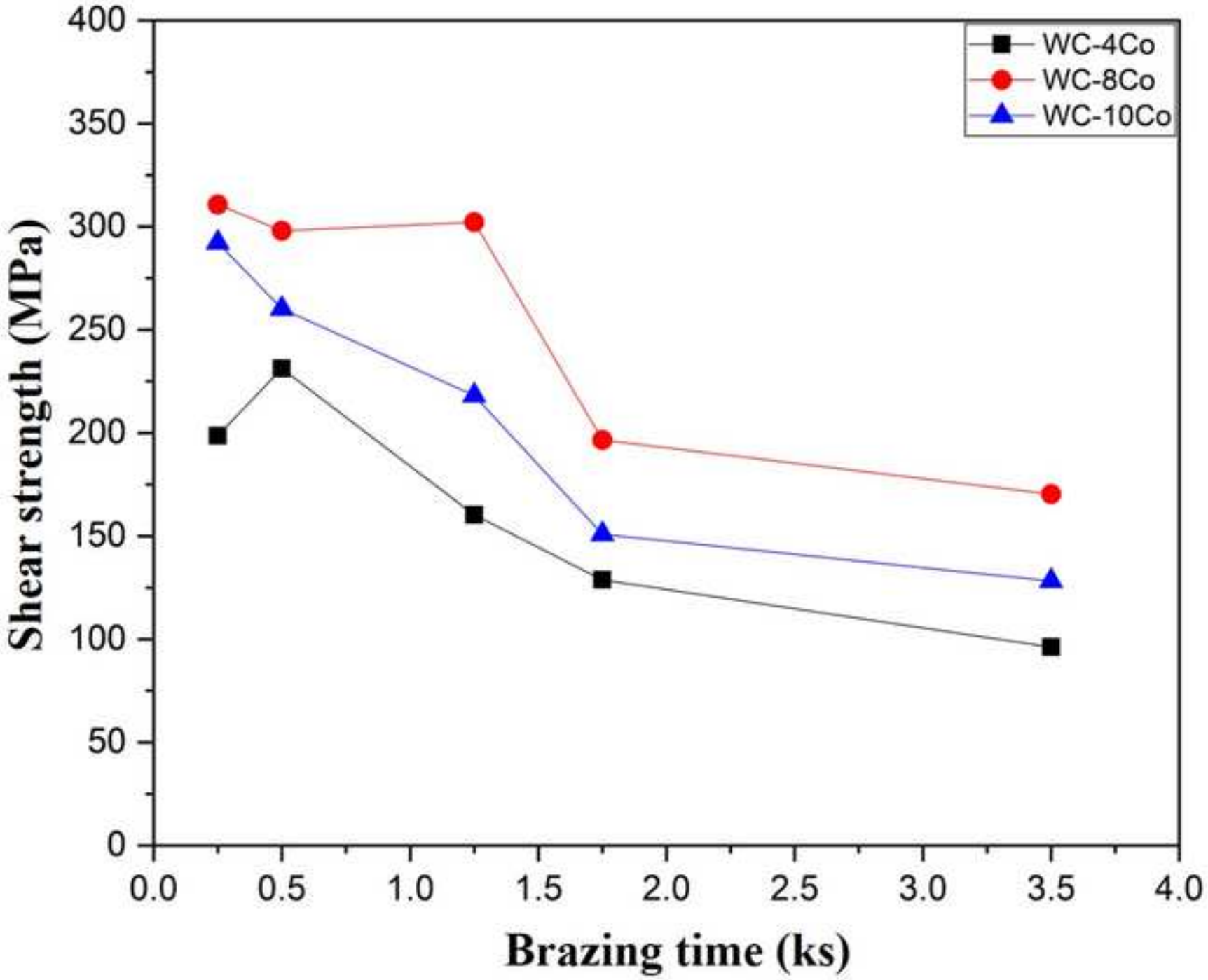

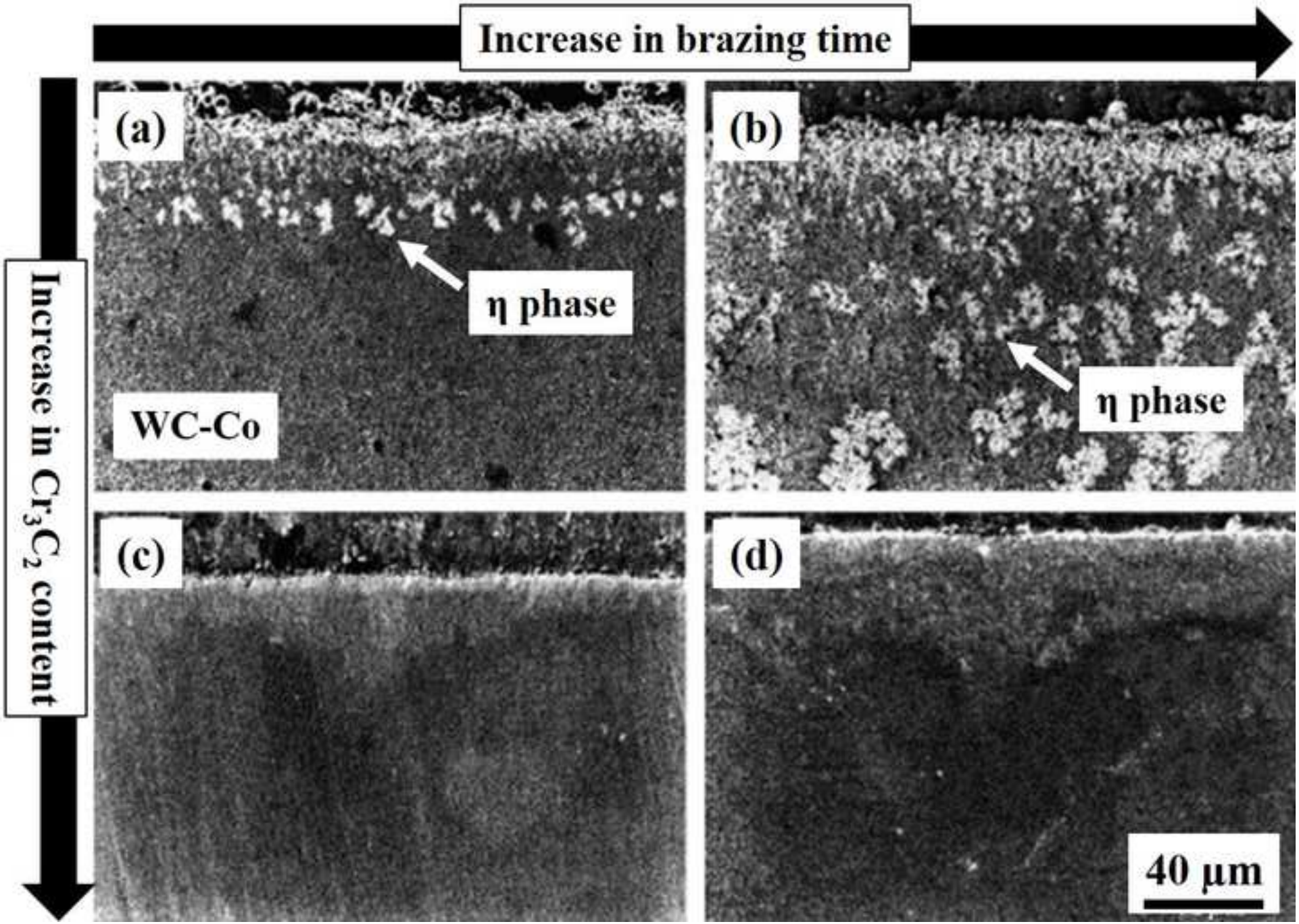

Colour figure

Click here to access/download;Colour figure;Fig 16.jpg

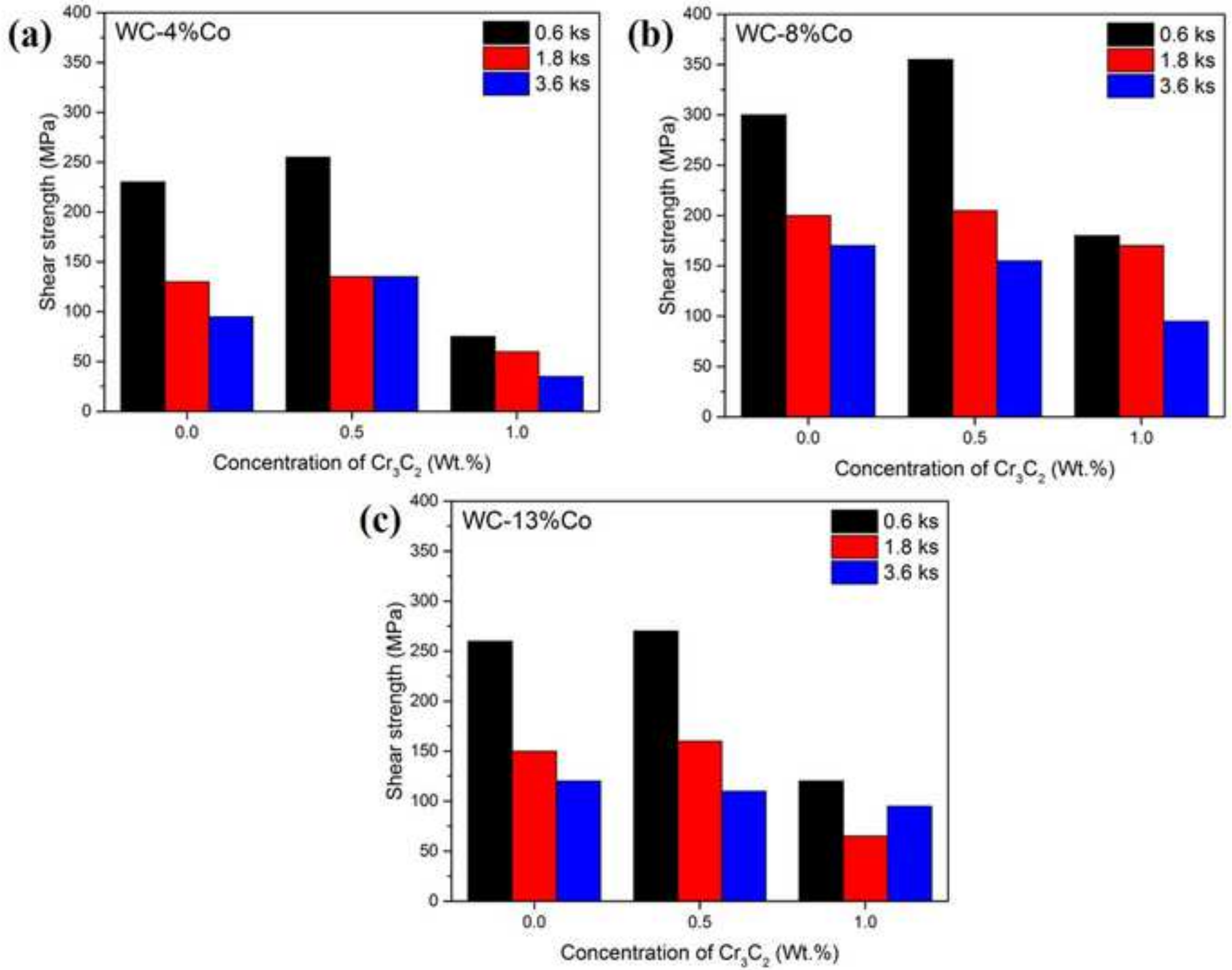

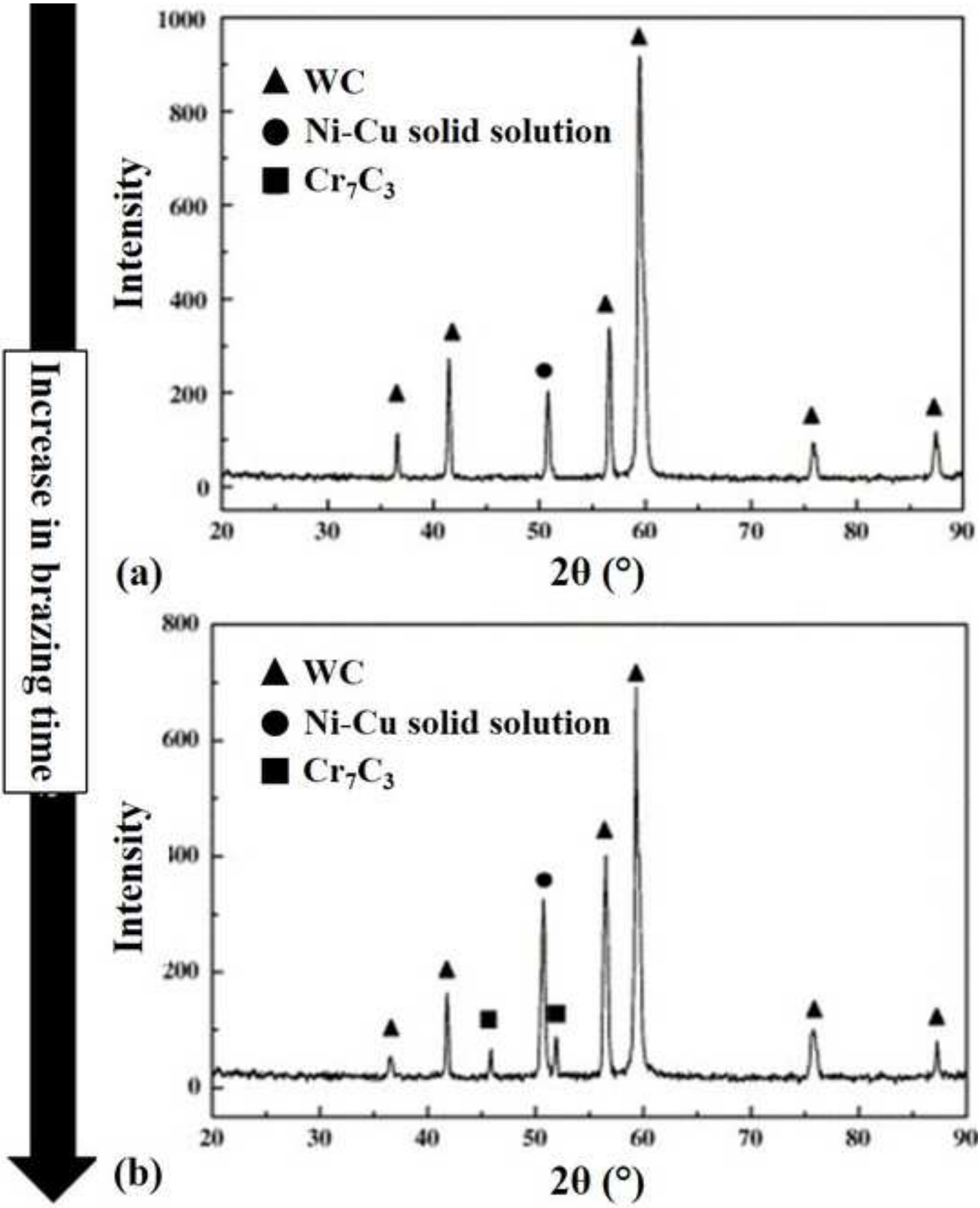

Non-colour figure

Click here to access/download;Non-colour figure;Fig filler.jpg